

THE MODEL OF DEFORMING MODE TUBE UNDER  
AXIAL LOADING



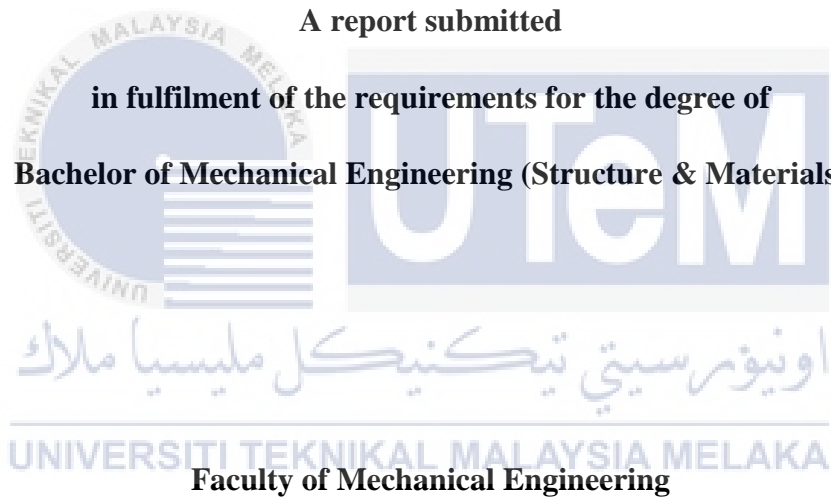
UNIVERSITI TEKNIKAL MALAYSIA MELAKA

**THE MODEL OF DEFORMING MODE TUBE UNDER  
AXIAL LOADING**

**MUHAMAD SYAFIQ BIN ABDUL WAHAB**

**A report submitted**

**in fulfilment of the requirements for the degree of  
Bachelor of Mechanical Engineering (Structure & Materials)**



**Faculty of Mechanical Engineering**

**UNIVERSITI TEKNIKAL MALAYSIA MELAKA**

**2017**

## APPROVAL

I hereby declare that I have read this project report and in my opinion this report is sufficient in terms of scope and quality for the award of the degree of Bachelor of Mechanical Engineering (Structure & Materials).



Signature : .....

Supervisor's Name : PROF. DR. MD. RADZAI BIN SAID

Date : .....

اونيورسيتي تيكنيكل مليسيا ملاك

---

UNIVERSITI TEKNIKAL MALAYSIA MELAKA

## DECLARATION

I declare that this project report entitled “The model of deforming mode tube under axial loading” is the result of my own work except as cited in the references.



## DEDICATION

To my beloved family especially my father, Abdul Wahab Bin Bujang and my mother, Ah  
Binti Haji Dali.



## ACKNOWLEDGEMENTS

Alhamdulillah, all praises to Allah for the strengths and His blessing in completing this search. To the great prophet Muhammad (Allah peace be upon him) a prophet of mercy and the light of the Worlds.

Firstly, I would like to sincerely thank my supervisor Prof. Dr. Md Radzai Bin Said for his guidance, advices and support. Without his valuable assistance, this work would not has been completed. I am also indebted to my friends for their contributions. I takes this opportunity also to thank the Faculty of Mechanical Engineering's laboratory management for their cooperation especially to the technicians during performing experimental works at the laboratory.

Most importantly, I am forever grateful my family who understands the importance of this work, none of this would have been possible without their patience and help.

Lastly, specials thanks are due to all who was has involved in helping to finish this project.

UNIVERSITI TEKNIKAL MALAYSIA MELAKA

## ABSTRACT

Thin-walled tube is one of the energy absorbing structure that has been used to dissipate energy and increase the efficiency of crashworthiness. During an accident occurred, thin-walled tube dissipates the kinetic energy and convert it into other form of energy. Therefore, this energy absorbing structure gives enough energy dissipation before hitting the human. This study examines the square aluminium tube and circular Polyvinyl chloride (PVC) tube subjected to quasi static loading by using universal compression machine or Instron machine. The deforming modes for both tubes is observed. The paper model is developed by using a thick paper to illustrate the deforming mode for square aluminium tube only. Tensile test is conducted for both tubes in order to obtain the mechanical properties of the tubes. There are three difference in length for each types of tubes has been tested under quasi static loading. The experimental results obtained from the testing have been compared with theoretical results that obtained from mathematical equations. From the comparison, a good agreement has been achieved between the theoretical and experimental results. The analysis of load-displacement curve includes peak load, energy absorption, mean load and plastic folding results. Plastic folding for PVC tube is greater than aluminium tube because of the ductility behaviour. As a result, the circular PVC and square aluminium tubes deformed in progressive diamond mode for all three difference length. A series of paper model is developed for various stage of the deformation process in order to illustrate the phenomenon of compression process of square aluminium tube occurred during testing. As a conclusion, the results obtained from this study such as the series of paper model for deforming mode of square tubes can be used as a new product of learning tools in order to increase the understanding about the phenomenon of compression test.

## **ABSTRAK**

*Tiub ber dinding nipis merupakan salah satu struktur menyerap tenaga yang telah digunakan untuk menyebarkan tenaga dan meningkatkan kecekapan kebolehtahanan hentakan. Semasa kemalangan berlaku, tiub ber dinding nipis menyerap tenaga kinetik dan menukar kepada bentuk tenaga lain. Oleh itu, struktur menyerap tenaga ini memberikan penyerapan tenaga yang mencukupi sebelum memukul manusia. Kajian ini adalah untuk mengkaji tiub aluminium persegi dan tiub PVC bulat yang tertakluk kepada beban statik kuasi dengan menggunakan mesin mampatan universal atau mesin Instron. Mod perubahan bagi kedua-dua tiub diperhatikan. Model kertas dibentuk dengan menggunakan kertas tebal untuk menggambarkan cara perubahan bagi tiub aluminium persegi sahaja. Ujian tegangan dijalankan bagi kedua-dua tiub untuk mendapatkan sifat-sifat mekanik tiub. Terdapat tiga perbezaan panjang untuk setiap jenis tiub telah diuji di bawah beban statik kuasi. Keputusan eksperimen yang diperolehi daripada ujian telah dibandingkan dengan keputusan teori yang diperolehi daripada persamaan matematik. Dari perbandingan, satu persetujuan yang baik telah dicapai di antara keputusan teori dan ujikaji. Analisis terhadap graf jarak beban termasuk keputusan beban puncak, purata beban, penyerapan tenaga dan plastik lipatan. Lipatan plastik untuk tiub PVC adalah lebih besar daripada tiub aluminium kerana sifat kekenyalannya. Hasil daripada ujian, tiub PVC bulat dan aluminium persegi tiub berubah dalam mod diamond untuk ketiga-tiga perbezaan panjang. Siri model kertas dibentuk untuk pelbagai peringkat proses perubahan untuk menggambarkan fenomena proses pemampatan tiub aluminium persegi berlaku semasa ujian. Kesimpulannya, keputusan yang diperolehi daripada kajian ini seperti siri model kertas perubahan bentuk tiub aluminium segi empat sama akan digunakan sebagai alat bantu pembelajaran yang baru untuk meningkatkan kefahaman tentang fenomena ujian mampatan.*



## TABLE OF CONTENTS

|   | <b>PAGE</b> |
|---|-------------|
| <b>APPROVAL</b>   | <b>i</b>    |
| <b>DECLARATION</b>                                      | <b>ii</b>   |
| <b>DEDICATION</b>                                       | <b>iii</b>  |
| <b>ACKNOWLEDGEMENTS</b>                                 | <b>iv</b>   |
| <b>ABSTRACT</b>   | <b>v</b>    |
| <b>ABSTRAK</b>  | <b>vi</b>   |
| <b>TABLE OF CONTENT</b>                                 | <b>vii</b>  |
| <b>LIST OF TABLES</b>                                   | <b>x</b>    |
| <b>LIST OF FIGURES</b>                                  | <b>xi</b>   |
| <b>LIST OF ABBREVIATIONS</b>                            | <b>xiv</b>  |
| <b>LIST OF SYMBOLS</b>                                  | <b>xv</b>   |
| <b>CHAPTER</b>  |             |
| <b>1 INTRODUCTION</b>                                   | <b>1</b>    |
| 1.1 Background  | 1           |
| 1.2 Problem Statement                                   | 3           |
| 1.3 Objective   | 3           |
| 1.4 Scope Of Project                                    | 3           |
| <b>2 LITERATURE REVIEW</b>                              | <b>4</b>    |
| 2.1 Introduction  | 4           |
| 2.2 Energy Absorption                                   | 5           |
| 2.2.1 Collapse Modes                                    | 5           |
| 2.3 Quasi-Static Test                                   | 7           |
| 2.3.1 Axial Loading on Circular Polyvinylchloride (PVC) | 8           |
| 2.3.2 Axial Loading on Square Aluminium                 | 10          |
| 2.4 Globally Buckle                                     | 10          |

|          |   |    |
|----------|---|----|
| 2.5      | Paper Models of Deformation Modes   | 12 |
| 2.6      | Low Speed Camera  | 14 |
| <b>3</b> | <b>METHODOLOGY</b>  | 15 |
| 3.1      | Introduction  | 15 |
| 3.2      | Flow Chart for Tensile Test   | 16 |
| 3.3      | Material Selection for Tensile Test   | 17 |
| 3.4      | Material Preparation for Tensile Test                                       | 16 |
| 3.4.1    | Engineering Drawing for Tensile Test  | 19 |
| 3.4.2    | Cutting Process of Tensile Test Specimen                                    | 20 |
| 3.4.3    | Fabrication of Tensile Test Specimen  | 21 |
| 3.5      | Tensile Testing   | 22 |
| 3.6      | Flow Chart for Quasi Static Testing   | 23 |
| 3.7      | Material Selection For Quasi Static Testing                                 | 24 |
| 3.8      | Material Preparation for Quasi Static Testing                               | 25 |
| 3.9      | Experimental Setup for Quasi Static Testing                                 | 27 |
| 3.10     | Develop a Paper Model Using Thick Paper                                     | 28 |
| <b>4</b> | <b>RESULT AND ANALYSIS</b>  | 30 |
| 4.1      | Introduction  | 30 |
| 4.2      | Tensile Test  | 31 |
| 4.2.1    | Graph Tensile Stress Against Tensile Strain                                 | 31 |
| 4.2.2    | Experimental Tensile Testing Result   | 33 |
| 4.3      | Type of Deforming Modes for Aluminium and PVC Tubes under Quasi Static Test | 34 |
| 4.3.1    | Deforming Modes for Aluminium Tubes under Quasi Static Test                 | 34 |
| 4.3.2    | Deforming Modes for PVC Tubes under Quasi Static Test                       | 36 |
| 4.4      | Quasi Static Test Result  | 37 |
| 4.4.1    | Square Aluminium Tube with Length 100mm                                     | 37 |
| 4.4.1.1  | Comparison Between Experimental and Theoretical Value for Aluminium Tube    | 39 |

|          |  |           |
|----------|--|-----------|
|          | with Length 100mm  |           |
| 4.4.2    | Square Aluminium Tube with Length 150mm  | 41        |
| 4.4.2.1  | Comparison Between Experimental and<br>Theoretical Value for Aluminium Tube<br>with Length 150mm | 43        |
| 4.4.3    | Square Aluminium Tube with Length 200mm  | 45        |
| 4.4.3.1  | Comparison Between Experimental and<br>Theoretical Value for Aluminium Tube<br>with Length 200mm | 48        |
| 4.4.4    | Sample Calculation for Square Aluminium<br>Tubes   | 50        |
| 4.4.5    | Circular PVC Tube with Length 100mm  | 52        |
| 4.4.5.1  | Comparison Between Experimental and<br>Theoretical Value for PVC Tube with<br>Length 100mm       | 54        |
| 4.4.6    | Circular PVC Tube with Length 150mm  | 56        |
| 4.4.6.1  | Comparison Between Experimental and<br>Theoretical Value for PVC Tube with<br>Length 150mm       | 58        |
| 4.4.7    | Circular PVC Tube with Length 200mm  | 60        |
| 4.4.7.1  | Comparison Between Experimental and<br>Theoretical Value for PVC Tube with<br>Length 200mm       | 63        |
| 4.4.8    | Sample Calculation for Circular PVC Tubes  | 65        |
| 4.5      | Paper Model For Square Aluminium Tube  | 67        |
| <b>5</b> | <b>CONCLUSION AND RECOMMENDATION</b>   | <b>69</b> |
| 5.1      | Introduction   | 69        |
| 5.2      | Conclusion   | 69        |
| 5.3      | Recommendation   | 70        |
|          | <b>REFERENCES</b>  | <b>71</b> |
|          | <b>APPENDICES</b>  | <b>73</b> |

## LIST OF TABLES

| TABLE | TITLE  | PAGE |
|-------|--|------|
| 2.1   | Collapse modes under axial loading   | 5    |
| 4.1   | Experimental tensile testing result for aluminium  | 33   |
| 4.2   | Experimental tensile testing result for PVC  | 33   |
| 4.3   | Time taken for the tubes to compressed 60% from their total length   | 35   |
| 4.4   | Comparison between experimental and theoretical results of quasi-static testing for aluminium tube with length 100mm | 40   |
| 4.5   | Comparison between experimental and theoretical results of quasi-static testing for aluminium tube with length 150mm | 44   |
| 4.6   | Comparison between experimental and theoretical results of quasi-static testing for aluminium tube with length 200mm | 49   |
| 4.7   | Properties of square aluminium tubes   | 50   |
| 4.8   | Comparison between experimental and theoretical results of quasi-static testing for PVC tube with length 100mm       | 55   |
| 4.9   | Comparison between experimental and theoretical results of quasi-static testing for PVC tube with length 150mm       | 59   |
| 4.10  | Comparison between experimental and theoretical results of quasi-static testing for PVC tube with length 200mm       | 64   |
| 4.11  | Properties of circular PVC tubes   | 65   |

## LIST OF FIGURES

| FIGURE | TITLE  | PAGE |
|--------|--|------|
| 2.1    | Force displacement curve for collapse mode                                 | 6    |
| 2.2    | INSTRON 5585 testing machine   | 8    |
| 2.3    | PVC tubes on testing machine   | 9    |
| 2.4    | Local buckling at the upper part of the tubes                              | 9    |
| 2.5    | Collapse modes for aluminium square tubes                                  | 10   |
| 2.6    | Euler buckling deforming mode  | 11   |
| 2.7    | Theoretical model of a collapsing tube showing details of travelling hinge | 12   |
| 2.8    | Series of collapse mode and paper models                                   | 13   |
| 2.9    | Paper models of different in length  | 13   |
| 2.10   | Low speed digital video camera   | 14   |
| 3.1    | Schematic representation of general experimental setup                     | 15   |
| 3.2    | Flow chart of the testing  | 16   |
| 3.3    | Aluminium square tubes   | 17   |
| 3.4    | Polyvinylchloride (PVC) tubes  | 17   |
| 3.5    | Dimension of tensile test specimen for aluminium (ASTM E8)                 | 18   |
| 3.6    | Dimension of tensile test specimen for PVC (ASTM D638)                     | 19   |
| 3.7    | Drawing of tensile test specimen for aluminium                             | 19   |
| 3.8    | Drawing of tensile test specimen for PVC                                   | 20   |
| 3.9    | Laser cutting machine  | 20   |
| 3.10   | Tensile test specimen for PVC and aluminium                                | 21   |
| 3.11   | INSTRON 8872 testing machine and set up for tensile testing                | 22   |
| 3.12   | Flow chart for quasi static testing  | 23   |
| 3.13   | Aluminium square tubes   | 24   |

|      |  |    |
|------|--|----|
| 3.14 | PVC circular tubes   | 24 |
| 3.15 | Bandsaw machine  | 25 |
| 3.16 | Cutting process for aluminium tubes  | 26 |
| 3.17 | Cutting process for PVC tubes  | 26 |
| 3.18 | Three difference of height for aluminium and PVC tubes                       | 26 |
| 3.19 | Experimental set up for quasi static testing                                 | 27 |
| 3.20 | Manila paper   | 28 |
| 3.21 | The lines of folding and point of plastic hinges                             | 29 |
| 4.1  | Tensile test specimens break (aluminium and PVC)                             | 31 |
| 4.2  | Graph of tensile stress against tensile strain for aluminium                 | 32 |
| 4.3  | Graph of tensile stress against tensile strain for PVC                       | 32 |
| 4.4  | Aluminium tubes with three different length (100mm, 150mm, 200mm)            | 34 |
| 4.5  | PVC tubes with three different length (100mm, 150mm, 200mm)                  | 36 |
| 4.6  | Sample 1 of load displacement curve for the aluminium tube with length 100mm | 37 |
| 4.7  | Sample 1 of deforming mode for aluminium tube with length 100mm              | 38 |
| 4.8  | Sample 3 of load displacement curve for the aluminium tube with length 150mm | 41 |
| 4.9  | Sample 1 of deforming mode for aluminium tube with length 150mm              | 42 |
| 4.10 | Sample 1 of load displacement curve for the aluminium tube with length 200mm | 45 |
| 4.11 | Sample 1 of deforming mode for aluminium tube with length 200mm              | 46 |
| 4.12 | Sample 1 of load displacement curve for PVC tube with length 100mm           | 52 |
| 4.13 | Sample 1 of deforming mode for PVC tube with length 100mm                    | 53 |
| 4.14 | Sample 1 of load displacement curve for PVC tube with length 150mm           | 56 |
| 4.15 | Sample 1 of deforming mode for PVC tube with length 150mm                    | 57 |
| 4.16 | Global buckling for sample 2 with length 200mm                               | 60 |
| 4.17 | Sample 1 of load displacement curve for PVC tube with length 200mm           | 61 |
| 4.18 | Sample 1 of deforming mode for PVC tube with length 200mm                    | 62 |

|      |                                       |    |
|------|---------------------------------------|----|
| 4.19 | Top view of tube and paper model      | 67 |
| 4.20 | Series of photographs of paper models | 68 |



## LIST OF ABBEREVATIONS

|     |   |                          |
|-----|---|--------------------------|
| IEA | - | Impact Energy Absorption |
| PVC | - | Polyvinylchloride        |
| PC  | - | Personal Computer        |





## LIST OF SYMBOLS

|            |   |                                 |
|------------|---|---------------------------------|
| $P_{cr}$   | - | Critical Buckling Load          |
| $P_m$      | - | Mean Load                       |
| $E$        | - | Young's Modulus / Energy Absorb |
| $\sigma_u$ | - | Tensile stress at yield         |
| $I$        | - | Moment of Inertia               |
| $L$        | - | Length of Tubes                 |
| $S$        | - | Deformation                     |
| $H_m$      | - | Half plastic folding            |
| $t$        | - | Thickness                       |
| $\nu$      | - | Poisson Ratio                   |
| $OD / d$   | - | Outer Diameter                  |
| $mm$       | - | Millimetre                      |
| $w$        | - | Width                           |
| $LO$       | - | Overall Length                  |
| $WO$       | - | Overall Width                   |
| $GPa$      | - | Giga Pascal                     |
| $MPa$      | - | Mega Pascal                     |

## CHAPTER 1

### INTRODUCTION

#### 1.1 BACKGROUND

In recent time, the number of vehicles on the road has rapidly increased year by year due to the advanced technologies in automotive industry (Ahmad, 2009). Afterward, vehicle crushing become a major worldwide problem that claimed many lives of road users. This phenomenon occurred due to high impact from the crushing on the body of vehicles to human body. Nowadays, impact energy absorption (IEA) device has contributed much in reduce of damage occurred on the bumper or body of vehicles during crushing especially in automotive or aerospace industries. The impact energy absorption (IEA) devices are expendable mechanical structural elements which are will action in the event of unwanted collision. IEA devices are single shot devices which is have to be replaced after they has been used for their purpose such as collision or crushing.

Polyvinylchloride (PVC) and aluminium are most popular material that are suitable in making the IEA device. This is because the material provide significant benefit such as high strength and durability, lightweight materials and lower in cost of processing or machining process. PVC was introduced in industry on 1832 and the first PVC pipes and tubes were produced on 1932 using a roll mill and hydraulic extruder (Pled et al., 2007). While, the first aluminium was produced in 1885 that containing iron and copper (Sheasby & Pinner, 2001). Too many application using this material due to low density and high mechanical strength.

One of the testing to deform the PVC and aluminium tubes is by using quasi-static testing (Ahmad, 2009). In this testing, the tubes are compressed at a constant rate using conventional tensional testing machine (INSTRON 8802). Tubes are compressed at a very slow constant speed in range of 0.0015 m/s up to 0.1 m/s. The height of the collapse modes of the tubes depend on the long of the tube before testing (Meng et al., 1983).

The results of collapse modes for both materials will be modelling by using a thick paper as a purpose of learning tools. Manila paper has been choose as a modelling material because of the lower in cost, accessible and also easy to handle in making of modelling of the collapse tubes. This paper typically made from semi-bleached wood fibres. It not as strong as craft paper but it most suitable paper in making of paper model of the deforming mode of the tubes. Paper model is describing the pattern or deforming mode of the tubes occurred from starting until the end of the tubes undergoes testing. Paper model will shows how the phenomena of the movement of the plastic hinges on the sides and the middle parts of the tubes. The movement of the plastic hinges is started from the tubes start to collapse under the apply load until the tubes is completely collapse. Only square in shape of the paper model will be modelling by using a thick paper as a purpose of teaching tools.

## 1.2 PROBLEM STATEMENT

One of the objective of this topic is expose to the students on how the deforming modes occurred on the tubes after undergoes an impact test. Nowadays, additional tools is needed to understand on how the phenomena of the deforming mode of the tubes occurred during the testing. So, study and research about the properties of PVC and aluminium is needed in identifying the behaviour of deforming modes for both materials. Then, modelling the results of the deforming mode for square aluminium tubes only by using thick paper which it can be used as a teaching and learning purpose. The series of paper model is developed for presentation in order to increase the understanding of students on phenomenon occurred during compression test is various stages.

## 1.3 OBJECTIVE

The objectives of this project are as follows:

1. To perform and observe the deforming mode of PVC and aluminium tubes with different length under quasi-static loading.
2. To model the deforming mode of the square aluminium tube only by using a thick paper.

## 1.4 SCOPE OF PROJECT

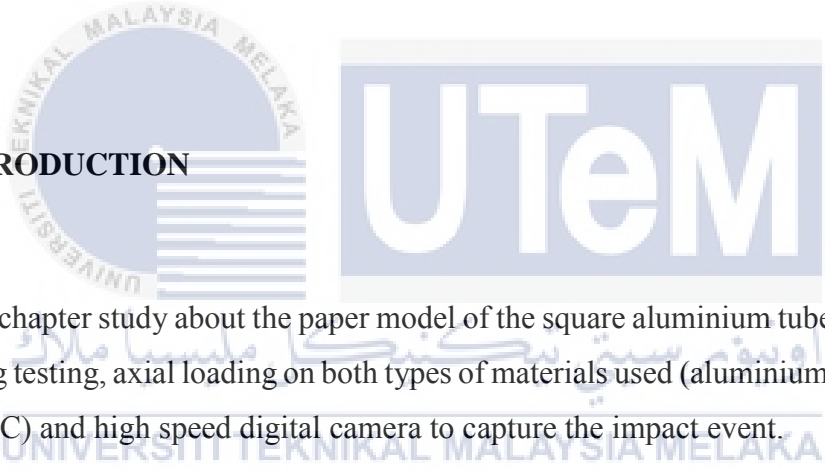
The scopes of this project are:

1. Carry out a preliminary study and review past research on the scope of study about quasi-static loading and deforming modes which is based on standard.
2. Perform a quasi-static loading on PVC and aluminium tubes and observe their deforming mode.
3. Result of deforming mode for square aluminium tube only are modelling by using the thick paper.

## CHAPTER 2

### LITERATURE REVIEW

#### 2.1 INTRODUCTION



This chapter study about the paper model of the square aluminium tubes under quasi-static loading testing, axial loading on both types of materials used (aluminium and polyvinyl chloride, PVC) and high speed digital camera to capture the impact event.

Axial loading of the tubes becomes one of the major part of the energy absorbing process employed by the designer. There are many publications on the behaviour of circular and square tubes under axial loading. From the view of energy absorption capacity, circular tubes under axial loading provide a better device compared with square tube (Meng et al., 1983).

## 2.2 ENERGY ABSORPTION

Energy absorption means that the required energy to cause the collapse of the structures or tubes under the impact loading (Andrews et al., 1983). The energy firstly transformed into elastic strain energy in the deformed tubes and the remainder of the energy is dissipated in plastic deformation on the tubes during collapse occurred (Alghamdi, 2001). There are seven types of collapse modes on tubes that has been identified which are concertina, axisymmetric concertina, diamond, concertina/diamond, Euler, tilting of tube axis and 2-lobe diamond (Albert et al., 2016).

### 2.2.1 COLLAPSE MODES

Results from the axial loading to the test tubes produced seven types of collapse modes which is (Andrews et al., 1983):

Table 2. 1: Collapse modes under axial loading

| <b>Collapse modes</b>   | <b>Description</b>  |
|-------------------------|---|
| Concertina              | At one end of the tube where starting point of axisymmetric and sequential folding.                             |
| Axisymmetric concertina | Simultaneous type of collapse will occurred along the length of the tubes.                                      |
| Diamond                 | Change in the cross section shape of the tubes affected by the sequential folding.                              |
| Concertina / Diamond    | Folding first occurred in concertina mode and changing to diamond mode.   |
| Euler                   | Tubes bending during the testing.   |
| Tilting of tube axis    | Shearing occurred on the tubes with platen surface at the one end.  |
| 2-Lobe diamond          | Simultaneous type of collapse will occurred along the length of the tubes in form 2-lobe diamond configuration. |

There are four different regions in the force-displacement curve for the collapse mode as shown in the Figure 2.1 which is the post-buckling stage, elastic stage, the crippling stage and the collapse stage.

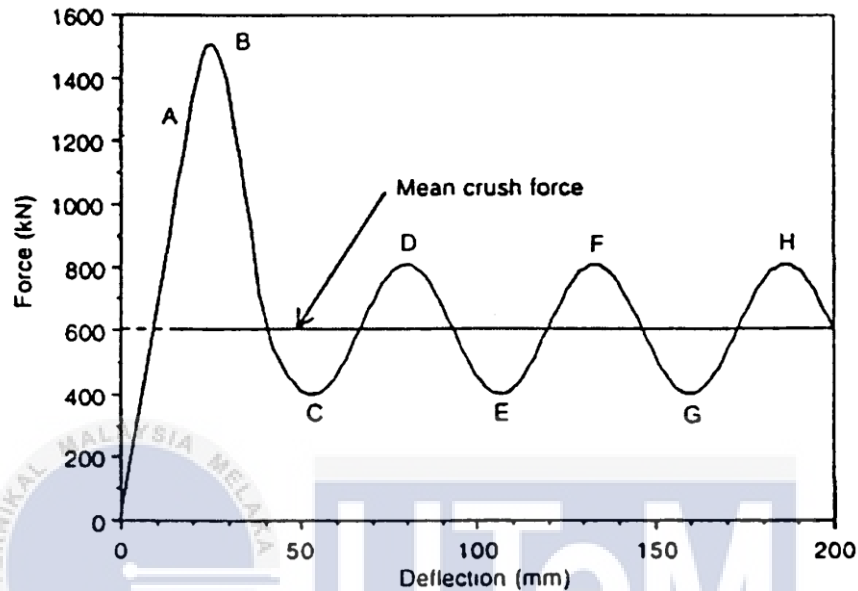


Figure 2. 1: Force displacement curve for collapse mode  
(Source : Junning Sun, 2000)

According to the Figure 2.1, point A represented the elastic buckling load. For the point B, it is referred to maximum crippling load means that the maximum load-carrying capacity of the tube. This point also indicated as maximum peak force for the testing where at the corners of the tubes, plastic collapse will happened. As the applied loads is decreases to the point C, the first fold is appeared at the corner of the tubes. When the load increasing, second crippling load is reached at point D. It is also followed by the loading increasing from the point E to F and G to H. the process of folding occurred at the corner of the tube is repeated from the point D to E and F to G until the folding happens at the end of the tubes (Junning Sun, 2000).

## 2.3 QUASI-STATIC TEST

The quasi-static test was carried out by using INSTRON 5585 testing machine (accuracy  $\pm 1\%$  of applied load) as shown in Figure 2.2. The plate at the lower part of the machine was fixed and not move (Trondheim, 2005). To ensure uniform load distribution of the test specimens, the load was applied through a rigid steel plate that connected to the hydraulic actuator. The friction between the rigid steel plate and the upper end surface of the test specimens is very important to prevent from any movement during the testing process. The axial load was applied at a constant speed during the testing which the speed in a range of  $1.5 \times 10^{-3}$  m/s to 0.1 m/s. The actual crush condition didn't be able represent by doing this quasi-static tests because during the crush, the structures of the tubes will dissipate energy over the entire period until the tubes are completely collapses. It means that the speed of the tests is one of the major factor influences on the capability of energy absorption. So, materials selection under the quasi-static tests are usually not represent the real performance of the structure in the event of a crash.

There are some advantages of the quasi-static tests (Junning Sun, 2000):

- i. Lower maintenance and reduce the risk of damage on the crosshead of the tubes.
- ii. Test's equipment usually easy to conduct and operate.
- iii. This test usually run to understand the different failure modes of the different materials used based on the crush rate.

There are some disadvantages of the quasi-static test:

- i. This quasi-static tests usually represent not an actual characteristic of the selected materials as a real performance of the structure in the event of a crash. This is because this test usually conducted to investigate the failure modes of the tubes.





Figure 2. 2: INSTRON 5585 testing machine

UNIVERSITI TEKNIKAL MALAYSIA MELAKA

### 2.3.1 AXIAL LOADING ON CIRCULAR POLYVINYLCHLORIDE (PVC)

This type of material which is Polyvinylchloride (PVC) are commonly used in exterior applications such as window profile and sliding because of the lower cost in production. PVC are classified as a long term behaviour material because has a good record of long term durability (Alhamati & Ghazali, 2007).

The PVC tubes is one of the best energy absorption devices that are investigated by many researchers. The behaviour of the tubes are determined from collapsing of the tubes under axial loading. This tubes was indicated that will produced non-axisymmetric diamond mode of deformation (Ejlertsson et al., 2000) after a testing.

Figure 2.3 shown the PVC tubes will be test under axial loading that are using an INSTRON 8500 machine. The failure or local buckling of the tubes are expected occur at the top or bottom of the tubes.

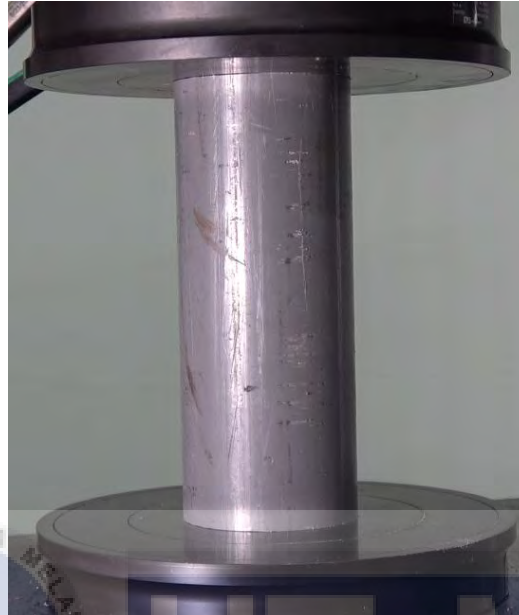


Figure 2.3: PVC tubes on testing machine  
(Source : Alhamati & Ghazali, 2007)

This is because the stress concentration around the external wall at this location (Alhamati & Ghazali, 2007). Figure 2.4 verified that the local buckling occurred at the upper part of the tube.

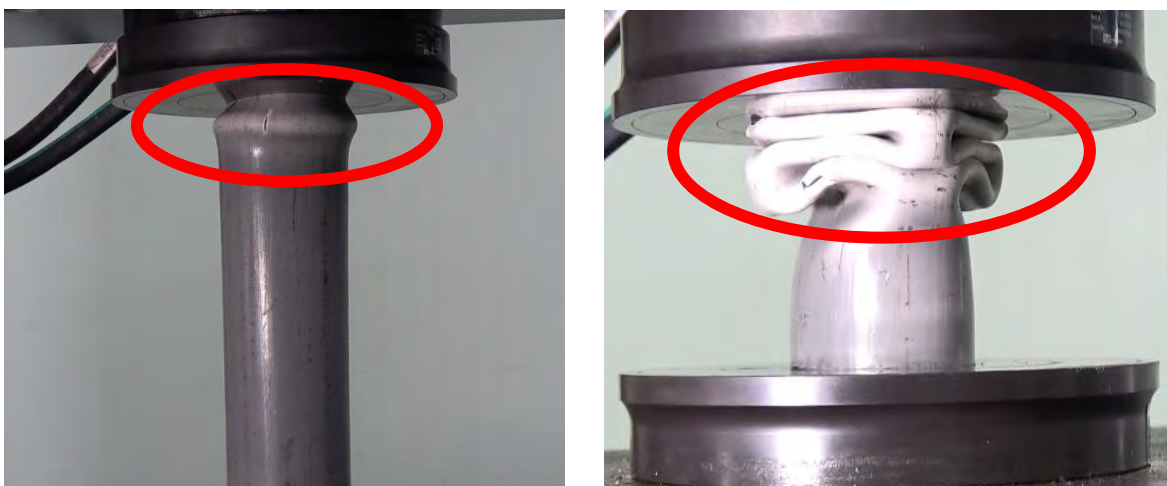


Figure 2. 4: Local buckling at the upper part of the tubes  
(Source : Alhamati & Ghazali, 2007)

### 2.3.2 AXIAL LOADING ON SQUARE ALUMINIUM

Square aluminium tubes are commonly used for reinforcement member of the structures (Miyazaki & Negishi, 2003). This aluminium tubes are suitable to be made as energy absorption devices especially in industry of automotive.

For the case of progressive buckling, the deformation of the tubes will starts with plate buckling in the extrusion wall (Trondheim, 2005). For all size of tubes thicknesses, a position of first lobe will appeared randomly along the length of the tubes. An axisymmetric collapse mode means that the two opposite extrusion walls move inwards and the others two wall of the tubes will move outwards. The deformation modes of a series of aluminium tubes (Meng et al., 1983) are shown in the Figure 2.5. The collapse modes of this tubes are more regular compared with collapse modes of PVC.



Figure 2. 5: Collapse modes for aluminium square tubes

(Source : Meng et al., 1983)

### 2.4 GLOBALLY BUCKLE

Euler buckling deformation produced when long tubes subjected to axial loading testing (Christy Albert et al., 2016). This phenomena occurred due to increase in length of the tubes. This collapse mode is classified by a large lateral displacements where induced the collapse at the middle and at the end of the tubes. Figure 2.6 shown the Euler buckling of the square aluminium tube.



Figure 2. 6: Euler buckling deforming mode

(Source : Christy Albert et al., 2016)

From the previous research (Ma, 2011), usually long square tubes tend to buckle globally which this phenomenon is called Euler buckling. The formula to calculate the critical buckling load of the long square tubes or slim member is shown in equation (2.1) below.

$$P_{cr} = \frac{\pi^2 EI}{L^2} \quad (2.1)$$

Based on this equation, E is Young's modulus, I is the moment of inertia of the cross section tubes and L is the length of the square tubes.

For circular tubes, the Euler buckling will occurred although the tubes is not long enough. The theory of (Timoshenko, 1961) indicated that the formula to calculate the critical buckling load is by using the equation (2.2) below.

$$P_{cr} = \frac{2\pi Et^2}{\sqrt{3(1-\nu^2)}} \quad (2.2)$$

Which t is the thickness of the tubes and  $\nu$  represent the Poisson ratio of the tubes.

## 2.5 PAPER MODELS OF DEFORMATION MODES

During the testing, the tubes will undergoes deformation. This is due to movement of plastic hinge at the middle part and corner of the tube. As shown in figure 2.7, the horizontal plastic hinge for a square tube is lies in the middle part of the tube in a direction which is perpendicular to the apply load (Meng et al., 1983).

Before start the testing, the location of the plastic hinge is at point BC. After the testing is started, the point of BC move to the point M'M and the last position of the plastic hinge is at point N'N. Complete one folding is produced when the point of plastic hinge reached at point N'N.

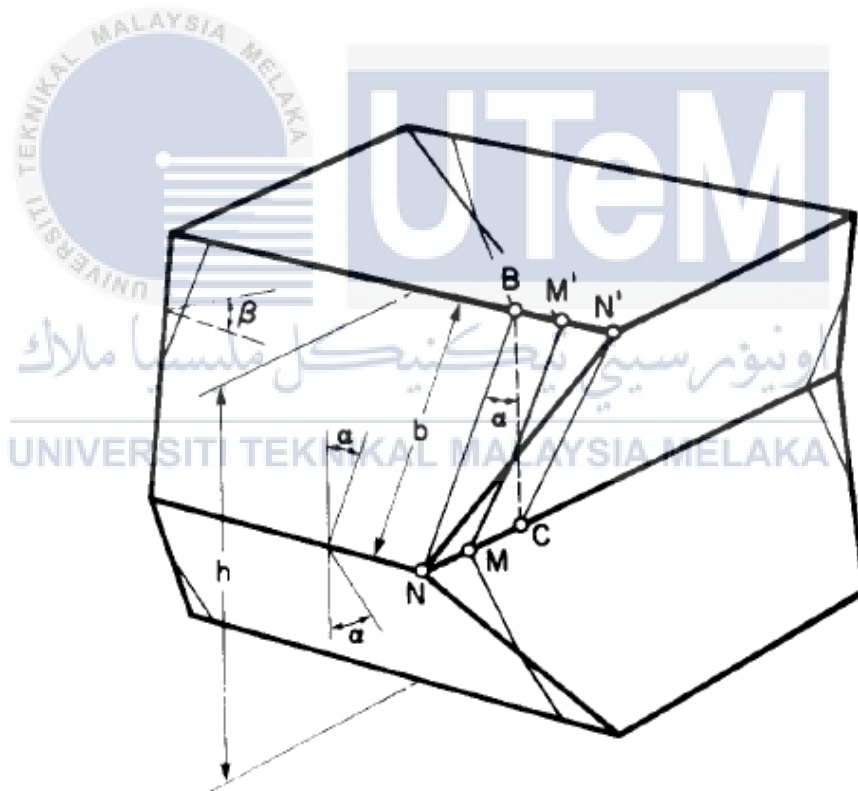


Figure 2. 7: Theoretical model of a collapsing tube showing details of travelling hinge  
( Source : Meng et al., 1983)

The deformation mode of the square tubes is shown by using a paper models. As shown in Figure 2.8, it demonstrated a series of collapse modes on the square tubes from the beginning until the end of the compression process. During the deformation, the top and bottom edges of the tube remain plane (Tai et al., 2010).

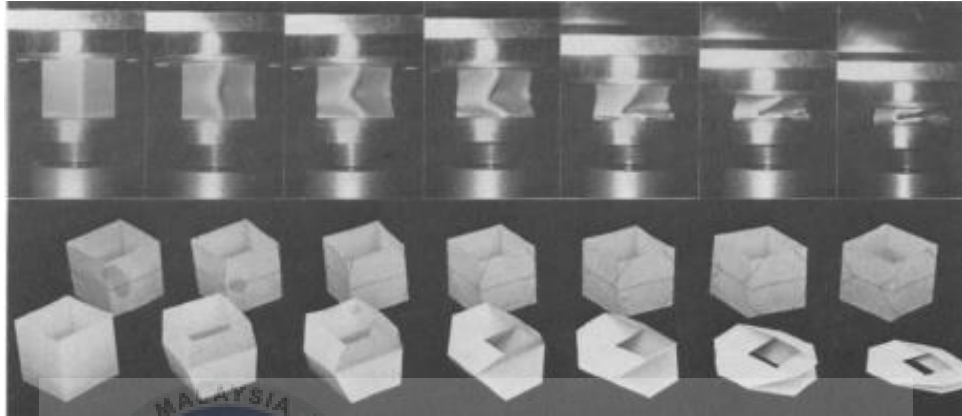


Figure 2. 8: Series of collapse mode and paper models

(Source : Meng et al., 1983)

For the case of longer tubes, the collapse modes was indicated consist a series of such collapse modes occurring one by one after another until the end top and bottom of the tubes (Meng et al., 1983). Figure 2.9 shown the two different of paper models between longer and shorter tubes after compression process.

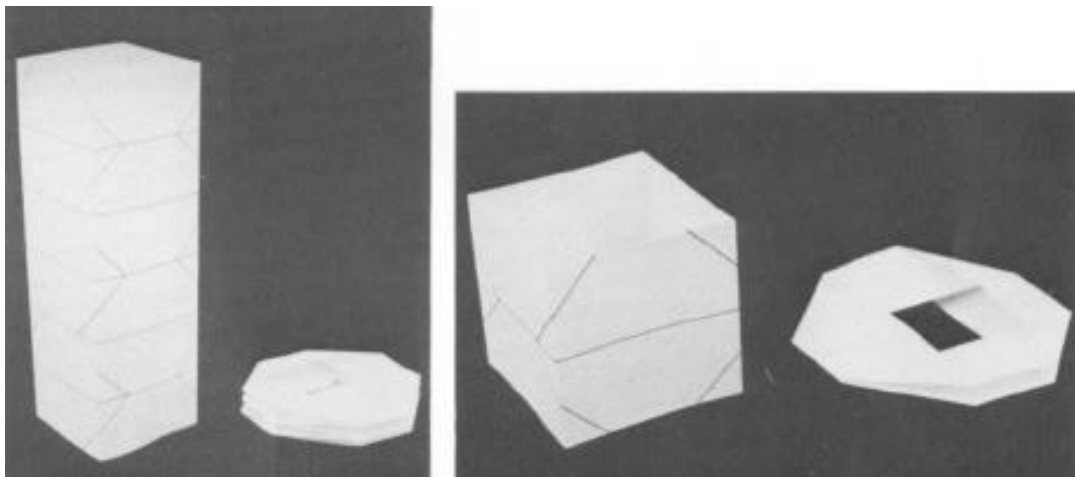


Figure 2. 9: Paper models of different in length

Figure 2. 9: (Source : Meng et al., 1983)

## 2.6 LOW SPEED CAMERA

A low speed digital video camera as shown in Figure 2.10 was used during the quasi-static testing on the test specimens to record the impact events, especially the global buckle and collapse behaviour of the specimen. This digital video camera offers a higher sensitivity and better image resolution than the colour model. During the impact tests, resolution of 512x1024 pixels were used that are produced maximum frame rate of approximately 2200 frames per second (Trondheim, 2005). The picture sequence of the experimental tests was stored in the memory of camera and transferred to a personal computer (PC) after the test.



Figure 2. 10: Low speed digital video camera

## CHAPTER 3

### METHODOLOGY

#### 3.1 INTRODUCTION

This chapter cover the material selection, material preparation for tensile test and tensile test on both materials which is aluminium and Polyvinylchloride (PVC). Besides, this chapter also cover the procedure of the compression test (quasi-test) on the both tubes. All the activities for this study are shown in Appendix A and Appendix B.

The general experimental setup of this project are shown in the Figure 3.1. The main objective of this setup is to obtain the collapse mode of both tubes. The purpose of using high speed digital camera is to capture the impact events during the quasi static tests. The videos and the pictures that has been recorded will be used in making of paper models of the collapse modes by using a thick paper.

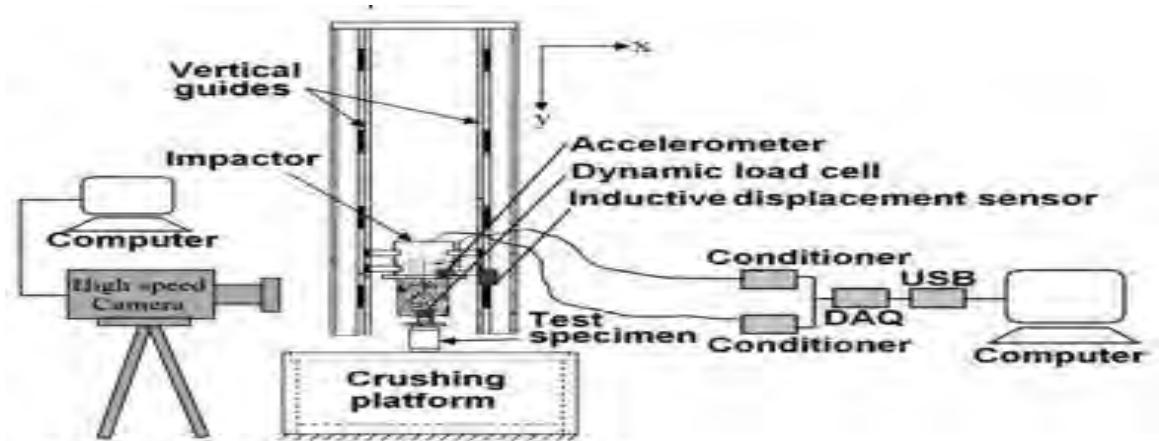


Figure 3. 1: Schematic representation of general experimental setup



### 3.2 FLOW CHART FOR TENSILE TEST

Based on the Figure 3.2 below, it shown a flow chart of the testing to conduct a tensile test for both material (aluminium and PVC). The purpose of this testing is to obtain the mechanical properties for both materials. This flow chart begin with literature review and followed by material selection, engineering drawing (AutoCad), tensile test specimen preparation, conduct a testing, analyse the results and report writing.

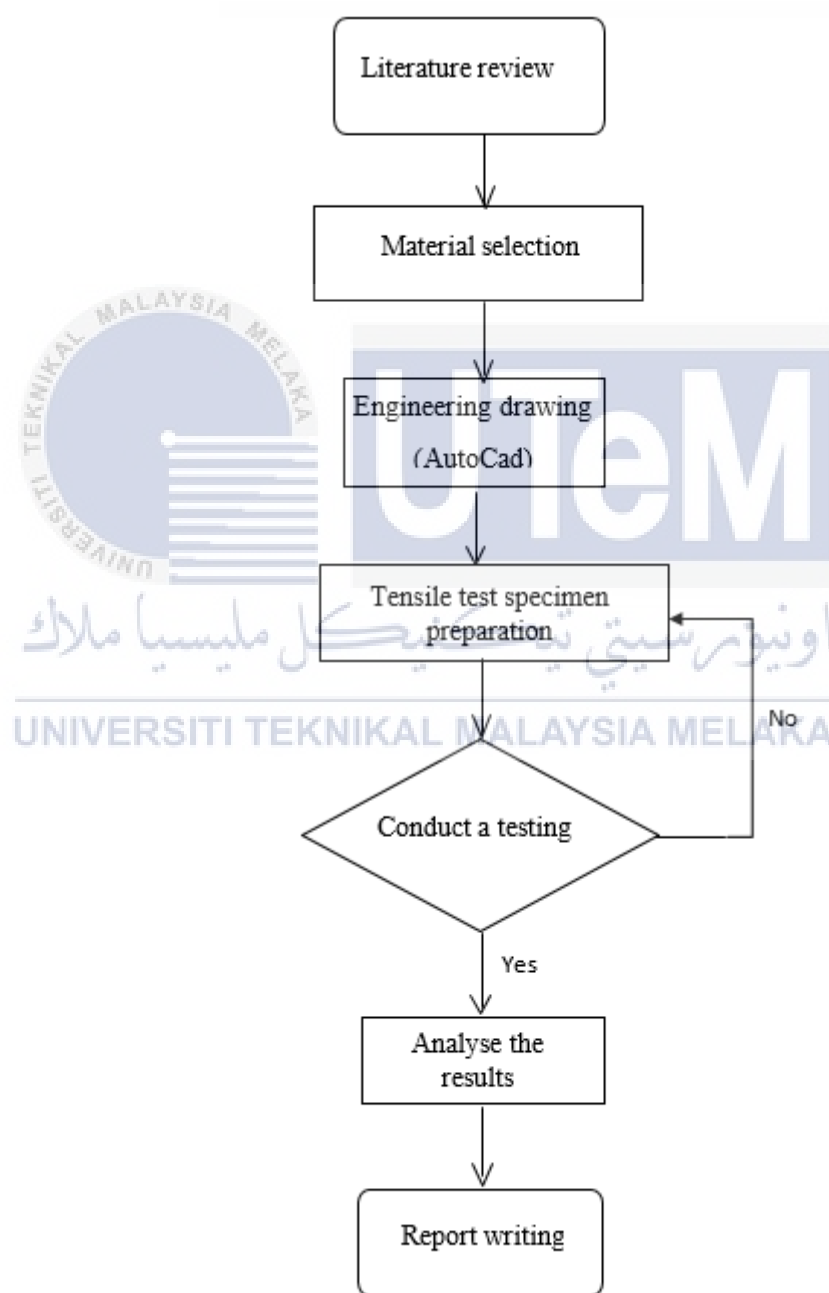


Figure 3. 2: Flow chart of the testing

### 3.3 MATERIAL SELECTION FOR TENSILE TEST

There are two types of material that has been used in preparation of tensile test specimen which is aluminium square tubes and Polyvinylchloride (PVC) tubes. For the aluminium square tubes, the length of the tubes needed to fabricate the tensile test specimen is 250mm, width of the tubes is 50.6mm and the thickness of the tubes is 1.1mm.



|                         |
|-------------------------|
| Length, $L = 250$ mm    |
| Width, $w = 50.6$ mm    |
| Thickness, $t = 1.1$ mm |

Figure 3. 3: Aluminium square tubes

Besides, for the PVC tubes, the required length of the tubes to fabricated tensile test specimen is 200mm, outer diameter of the tubes is 2.5 inch (63.5mm) and the thickness of the tubes is 2.6mm.



|                                |
|--------------------------------|
| Length, $L = 200$ mm           |
| Outer diameter, $OD = 63.5$ mm |
| Thickness, $t = 2.6$ mm        |

Figure 3. 4: Polyvinylchloride (PVC) tubes

### 3.4 MATERIAL PREPARATION FOR TENSILE TEST

Before that engineering drawing is drawn, the engineering standard reference for both materials need to study first. This is because to ensure that the tensile test for both materials is follow the engineering standard of the materials. Figure 3.5 and 3.6 shows the drawing and dimension for aluminium and PVC materials for tensile test specimen, respectively. The dimension that are stated in this figure will be used in drawing a tensile test specimen. The engineering standard for aluminium is ASTM E8 while for the PVC is ASTM D638.

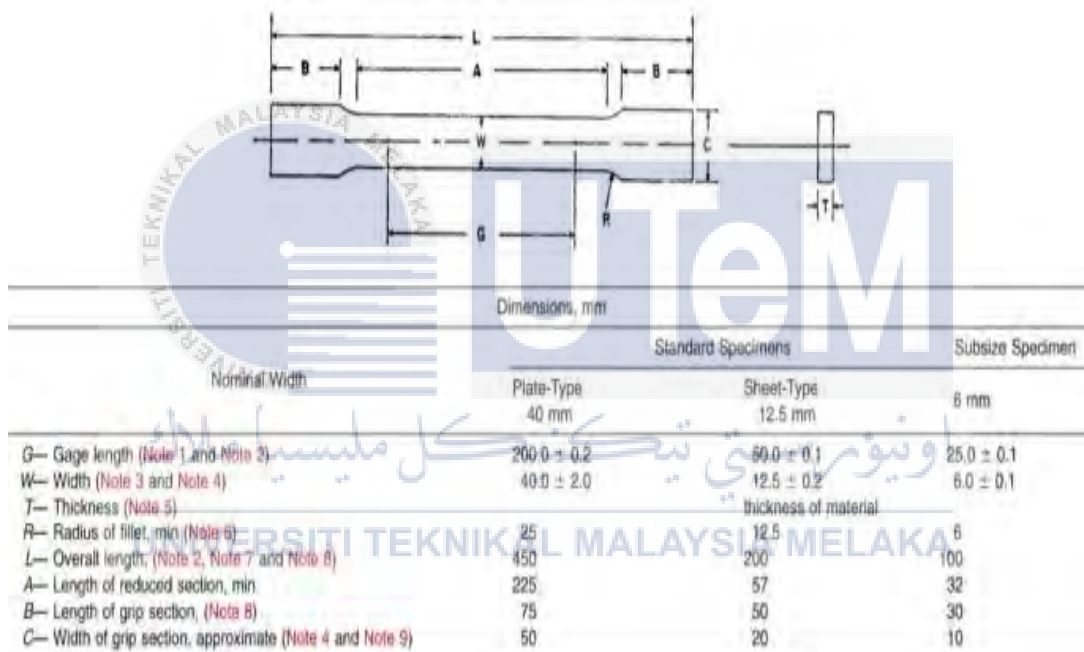
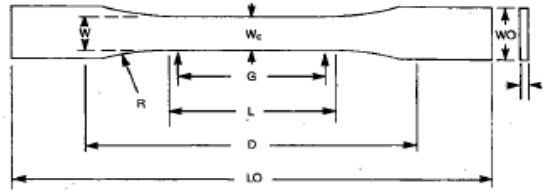
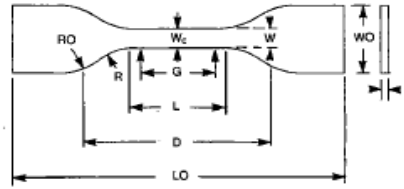


Figure 3. 5: Dimension of tensile test specimen for aluminium (ASTM E8)

(Source : ASTM Int., 2009)



TYPES I, II, III & V



TYPE IV

Specimen Dimensions for Thickness,  $T$ , mm (in.)<sup>A</sup>

| Dimensions (see drawings)                   | 7 (0.28) or under |           | Over 7 to 14 (0.28 to 0.55), incl | 4 (0.16) or under     |                       |
|---|-------------------|-----------|-----------------------------------|-----------------------|-----------------------|
|   | Type I            | Type II   | Type III                          | Type IV <sup>B</sup>  | Type V <sup>C,D</sup> |
| $W$ —Width of narrow section <sup>E,F</sup> | 13 (0.50)         | 6 (0.25)  | 19 (0.75)                         | 6 (0.25)              | 3.18 (0.125)          |
| $L$ —Length of narrow section               | 57 (2.25)         | 57 (2.25) | 57 (2.25)                         | 33 (1.30)             | 9.53 (0.375)          |
| $WO$ —Width overall, min <sup>G</sup>       | 19 (0.75)         | 19 (0.75) | 29 (1.13)                         | 19 (0.75)             | ...                   |
| $WO$ —Width overall, min <sup>G</sup>       | ...               | ...       | ...                               | ...                   | 9.53 (0.375)          |
| $LO$ —Length overall, min <sup>H</sup>      | 165 (6.5)         | 183 (7.2) | 246 (9.7)                         | 115 (4.5)             | 63.5 (2.5)            |
| $G$ —Gage length <sup>I</sup>               | 50 (2.00)         | 50 (2.00) | 50 (2.00)                         | ...                   | 7.62 (0.300)          |
| $G$ —Gage length <sup>I</sup>               | ...               | ...       | ...                               | 25 (1.00)             | ...                   |
| $D$ —Distance between grips                 | 115 (4.5)         | 135 (5.3) | 115 (4.5)                         | 65 (2.5) <sup>J</sup> | 25.4 (1.0)            |
| $R$ —Radius of fillet                       | 76 (3.00)         | 76 (3.00) | 76 (3.00)                         | 14 (0.56)             | 12.7 (0.5)            |
| $RO$ —Outer radius (Type IV)                | ...               | ...       | ...                               | 25 (1.00)             | ...                   |

Figure 3. 6: Dimension of tensile test specimen for PVC (ASTM D638)  
(Source : ASTM International, 2003)

### 3.4.1 ENGINEERING DRAWING FOR TENSILE TEST

After studying the standard for both materials, an engineering drawing for tensile test specimen is drawn by using CAD software which is AutoCad. Based on the Figure 3.7, it is shown the drawing of the tensile test specimen for aluminium material which is the overall length, LO of the specimen is 230mm and the overall width, WO is 20mm.

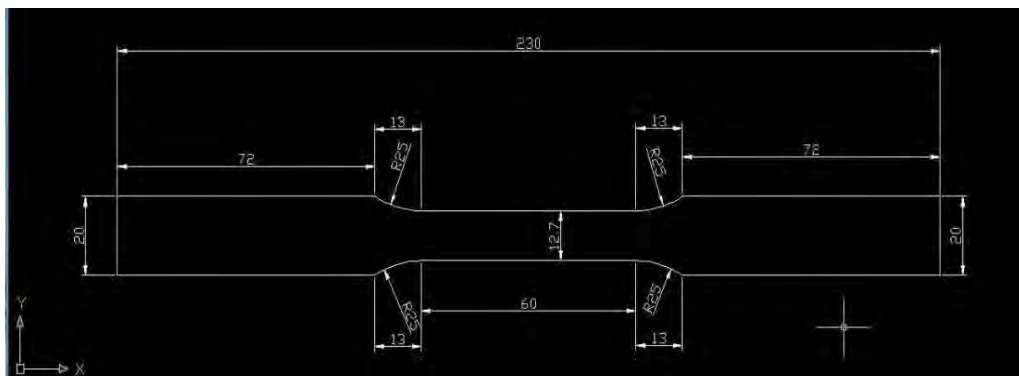


Figure 3. 7: Drawing of tensile test specimen for aluminium

By referring on the Figure 3.8 below, it is shown the drawing of the tensile test specimen for PVC material. The dimension of the drawing is based on the engineering standard which the overall length, LO of the specimen is 165mm and the overall width, WO is 19mm.

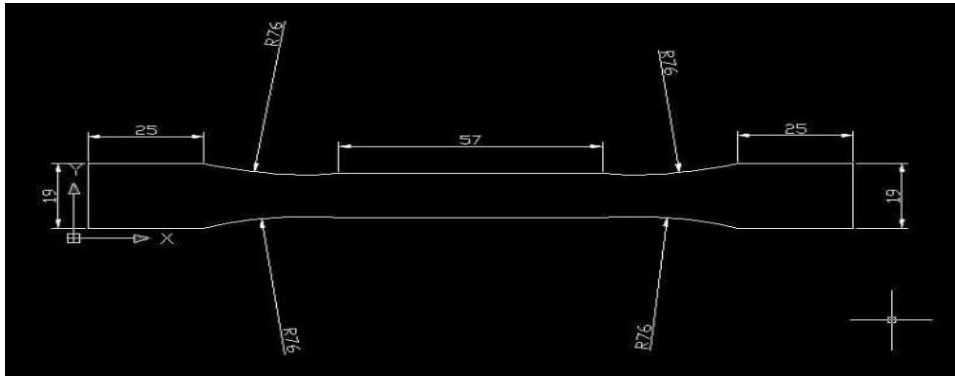


Figure 3. 8: Drawing of tensile test specimen for PVC

### 3.4.2 CUTTING PROCESS OF TENSILE TEST SPECIMEN

After the drawing of the tensile test specimen is done, both tubes need to cut by referring on the drawing. The action of cutting process will be done by using laser cutting machine as shown in the Figure 3.9. The coding of the drawing will be inserted into the computer of the machine and the machine will cut the tubes.

UNIVERSITI TEKNIKAL MALAYSIA MELAKA



Figure 3. 9: Laser cutting machine

Before running a cutting process, the hollow tube for both materials need to be filled up with a wooden block or solid steel known as blocker. The size of the blocker must smaller than the size of tubes to ensure that the blocker can fit up the hollow space of the tubes. The purpose of applying blocker inside the tubes is to prevent from the damage on opposite site wall of the tubes during cutting process.

### 3.4.3 FABRICATION OF TENSILE TEST SPECIMEN

The results of the cutting process are shown in Figure 3.10 for both materials. There are three pieces of specimen for each material has been cut as tensile test specimens. This is because during the tensile test, the testing need to run three times to get an accurate results by averaging the value of mechanical properties of the materials obtained from the testing.



Figure 3. 10: Tensile test specimen for PVC and aluminium

After cutting process, the tensile test specimen will produce rough surface around the cutting area especially for aluminium tubes. This is not necessary to apply finishing process on the surface. It is because during the cleaning process, it will change the microstructure of the specimen which can affect the result of the tensile test.

### 3.5 TENSILE TESTING

After fabrication of tensile test specimens is done, it will be test by using INSTRON 8872 testing machine and the set up for the testing are shown in Figure 3.11. The information obtained from the tensile test are:

- Tensile stress at maximum load.
- Tensile stress at yield.
- Tensile strain at break.
- Young's Modulus of the specimen

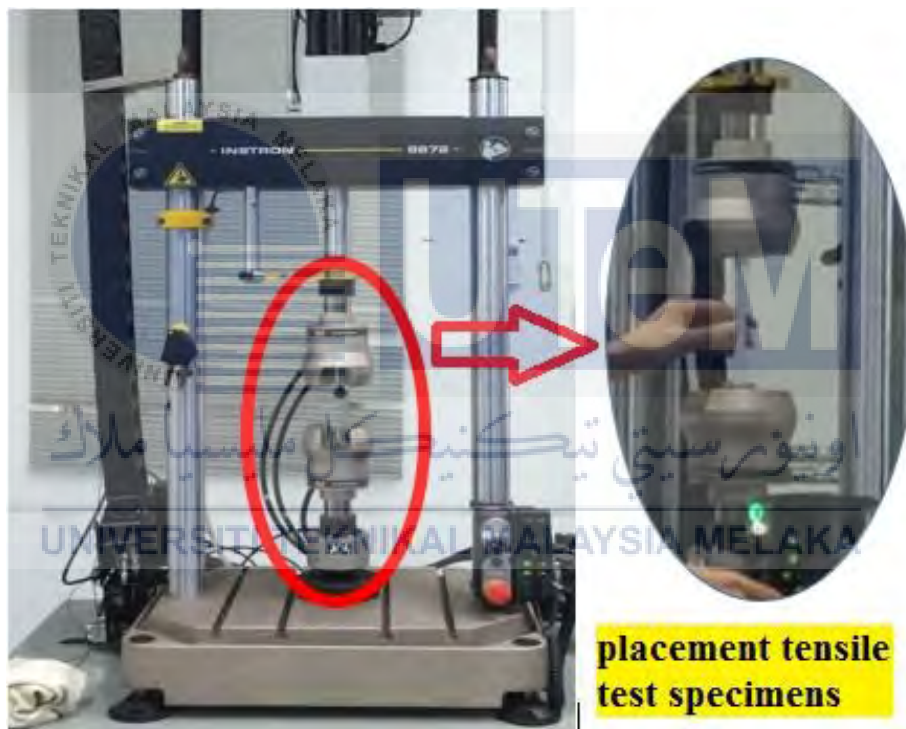


Figure 3. 11: INSTRON 8872 testing machine and set up for tensile testing

Before the testing started, the information such as length and the thickness of the tensile test specimen need to be inserted first on the computer. After that, the tensile test will start. During the testing, it takes a short time of a tensile test specimen to break due to soft materials and high speed of testing. The speed that has been used for this testing is 5mm / min.

### 3.6 FLOW CHART FOR QUASI STATIC TESTING

Based on the Figure 3.12 below, it shown a flow chart for quasi static testing for both materials (aluminium and PVC). The purpose of this testing is to obtain the types of deforming mode in three different length for both materials. This flow chart begin with literature review and followed by material selection, material preparation, conduct a testing, analyse the results and report writing.

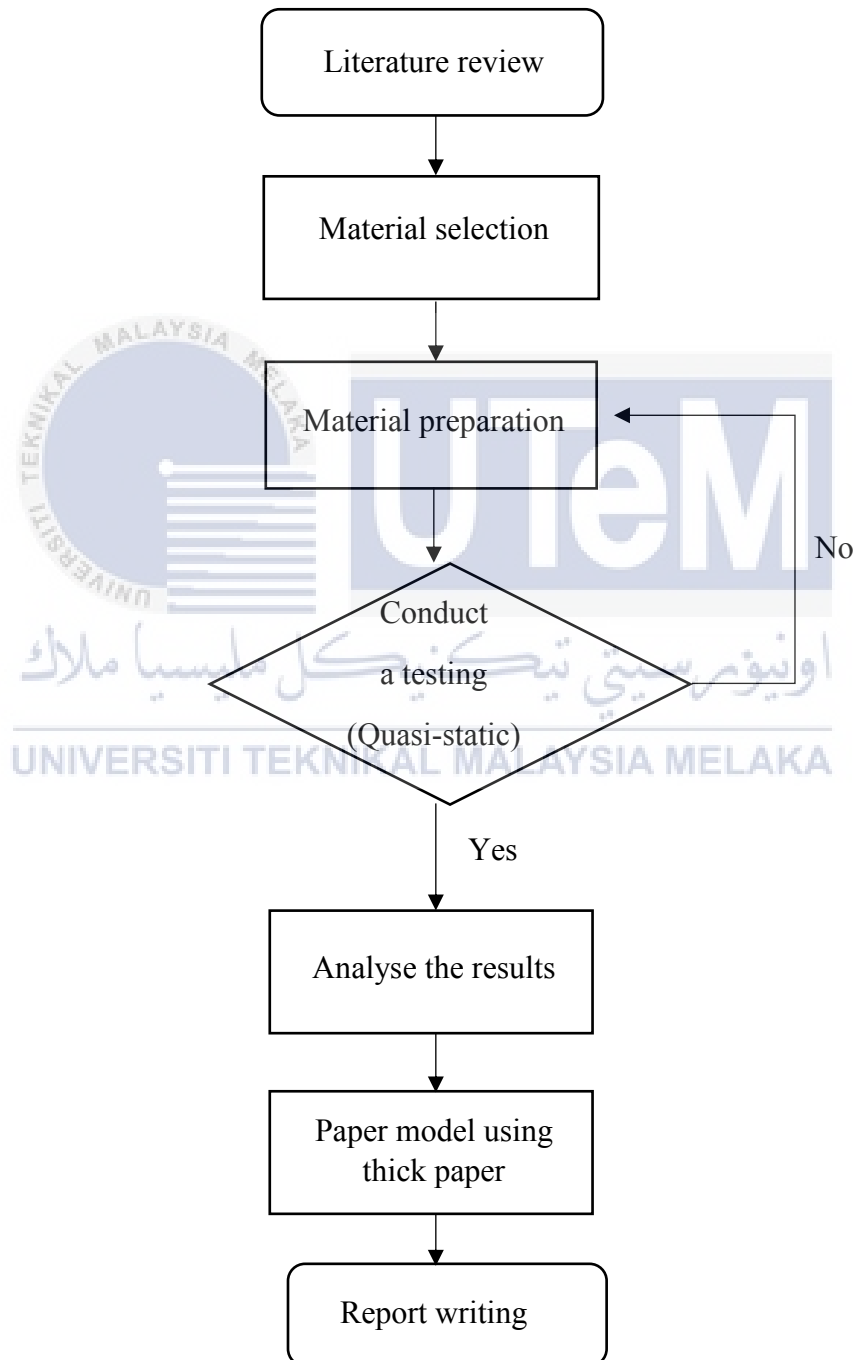


Figure 3. 12: Flow chart for quasi static testing.



### 3.7 MATERIAL SELECTION FOR QUASI STATIC TESTING

There are two types of material that has been used in preparation of quasi static testing which is aluminium square tubes and Polyvinylchloride (PVC) circular tubes. For the aluminium square tubes as shown in figure 3.13, the width of the tubes is 44.5mm and the thickness of the square tubes is 1.3mm.

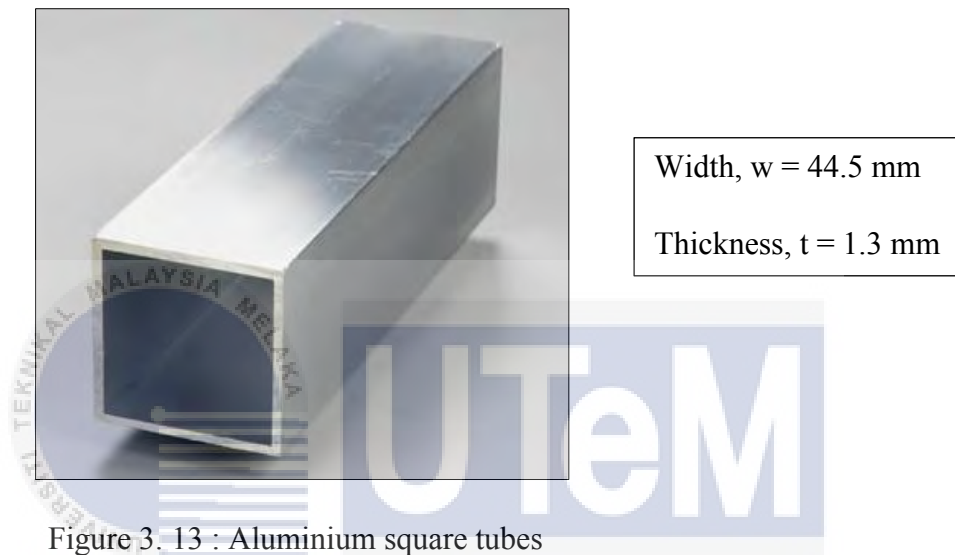


Figure 3. 13 : Aluminium square tubes

Besides, for the circular PVC tubes as shown in figure 3.14, the outer diameter of the tubes is 60.2mm and the thickness of the tubes is 2.9mm.

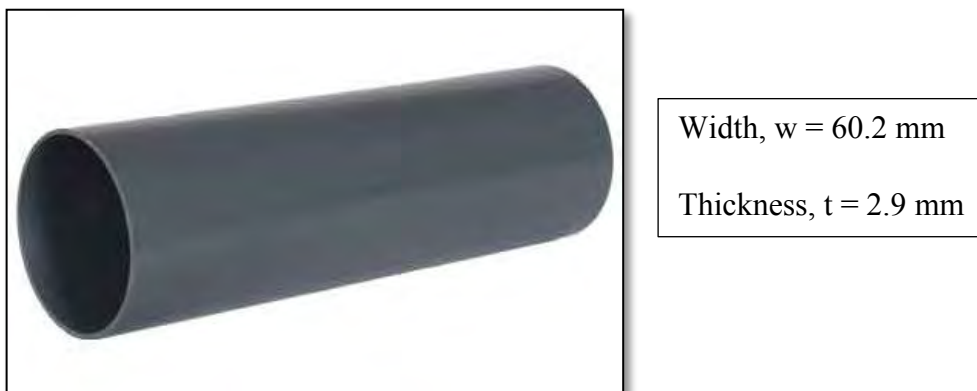


Figure 3. 14 : PVC circular tubes

### 3.8 MATERIAL PREPARATION FOR QUASI STATIC TESTING

There are three different of height for both materials will be prepared in this testing. Usually the tubes come out from production is about 5000mm in length and need to be cut by using a bandsaw machine as shown in the figure 3.15. This bandsaw machine is able to cut a raw materials such as aluminium, PVC, wood, mild steel and others.



Figure 3. 15 : Bandsaw machine

There are important to make sure that the tubes placed on the clamp is perpendicular with the sawn point in order to get perpendicular cutting surface with the length of the tubes. This is need to be considered because to prevent from slipping occurred between the tubes and the plates of testing machine during the quasi static testing. Besides, it also will affected the deforming modes of the tubes.

The cutting process for aluminium and PVC tubes are shown in figure 3.16 and figure 3.17 respectively. After finished the cutting process, surface of the cutting area need to be cleaned by using a file or sand paper in order to get a smooth surface.

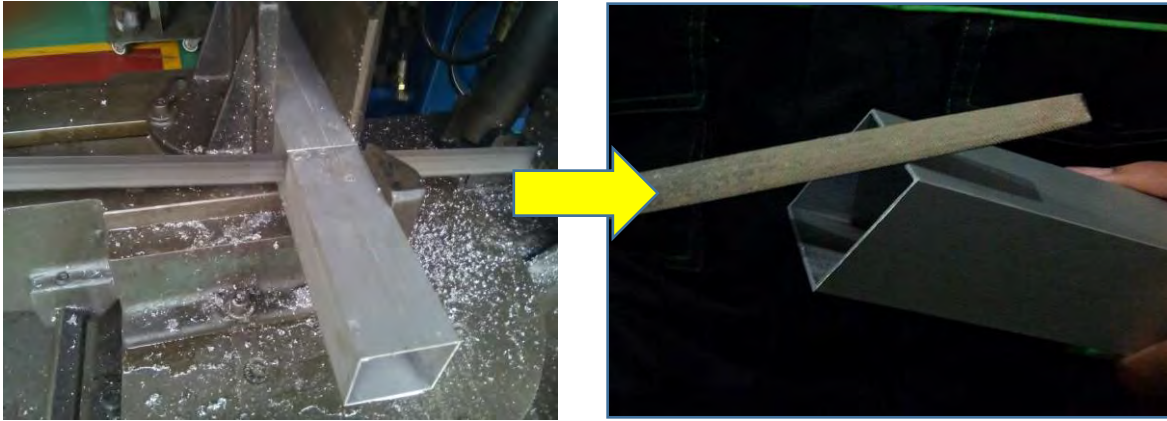


Figure 3. 16 : Cutting process for aluminium tubes

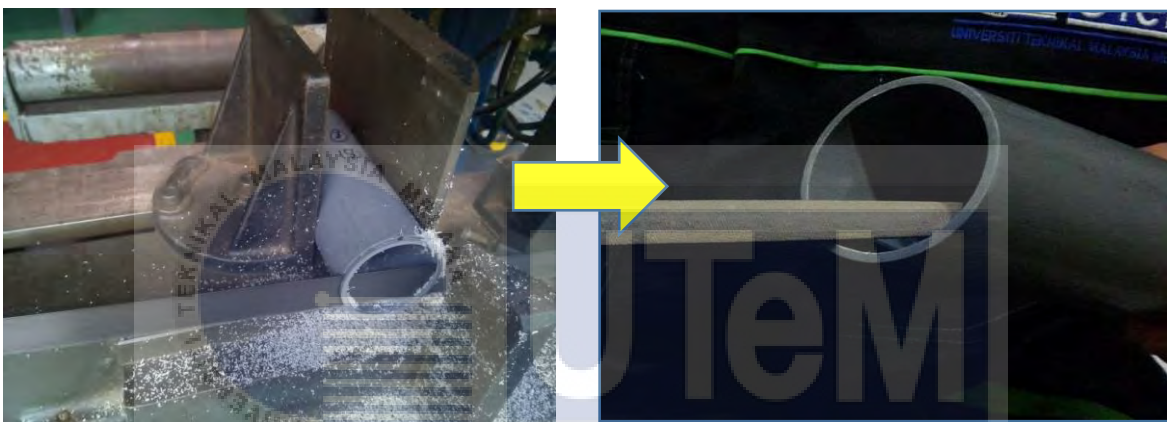


Figure 3. 17 : Cutting process for PVC tubes

The three different of height for aluminium and PVC tubes which are 100mm, 150mm and 200mm as shown in figure 3.18. For each height of tubes, there are 3 pieces of tubes has been prepared for quasi static testing.

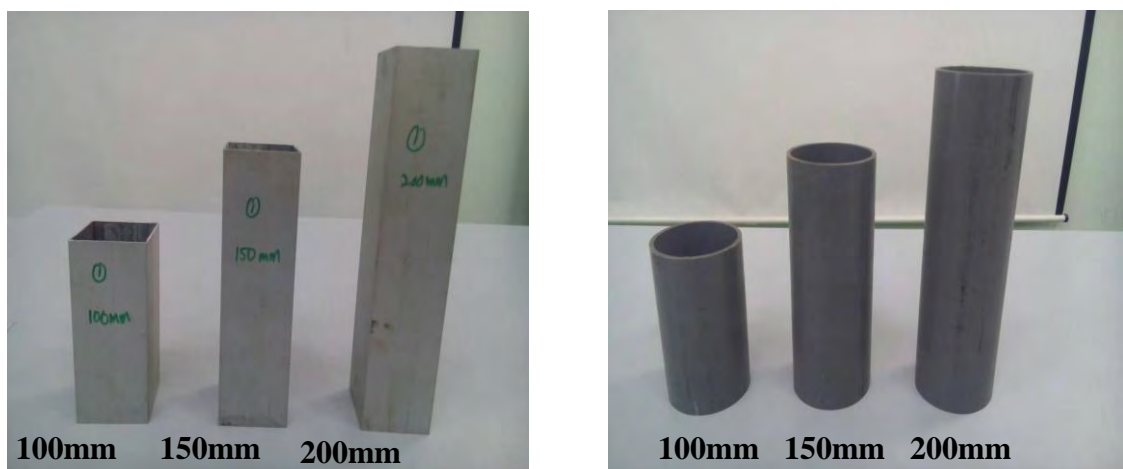


Figure 3. 18 : Three difference of height for aluminium and PVC tubes

### 3.9 EXPERIMENTAL SET UP FOR QUASI STATIC TESTING

The arrangement of the experimental set up for quasi static testing is shown in figure 3.19. This testing is performed using a standard universal testing (INSTRON) machine. Fundamental knowledge about the quasi static test is testing will be conducted at very slow speed of applied load. So, for this testing, the speed of the applied load that will be used is 10mm/min. The purpose of using low speed camera or handycam in this quasi static testing is to record the impact events, especially the phenomenon of deforming modes of the tubes during a testing. It will be used as reference to develop a paper model using a thick paper. In this experimental set up, sometimes LED light will be used in order to increase a light intensity of the testing area or laboratory during the testing.



Figure 3. 19 : Experimental set up for quasi static testing

The time taken for compress 60% from the total length of the tubes is about 6 minutes for 100mm tubes, 9 minutes for 150mm tubes and 12 minutes for 200mm tubes.

### 3.10 DEVELOP A PAPER MODEL USING THICK PAPER

The paper model are modelling using thick paper as a purpose of teaching tools. As shown in figure 3.20, Manila paper is chosen as modelling materials because it easy to handle in developing a paper model. It also not easily to torn during folding due their high thickness compared with plain paper. This Manila paper also readily available and have a variety in colour with smooth texture on the surface. The thickness of this paper that has been choose is 160gsm. The height and width of this paper is 410mm and 510mm respectively.



Figure 3. 20 : Manila paper

The lines of folding and point of plastic hinges has been drawn on this Manila paper as shown in figure 3.21. There are 5 point of plastic hinges drawn horizontally through the middle line of the paper shows the travelling of the plastic hinges due to increasing of applied load.

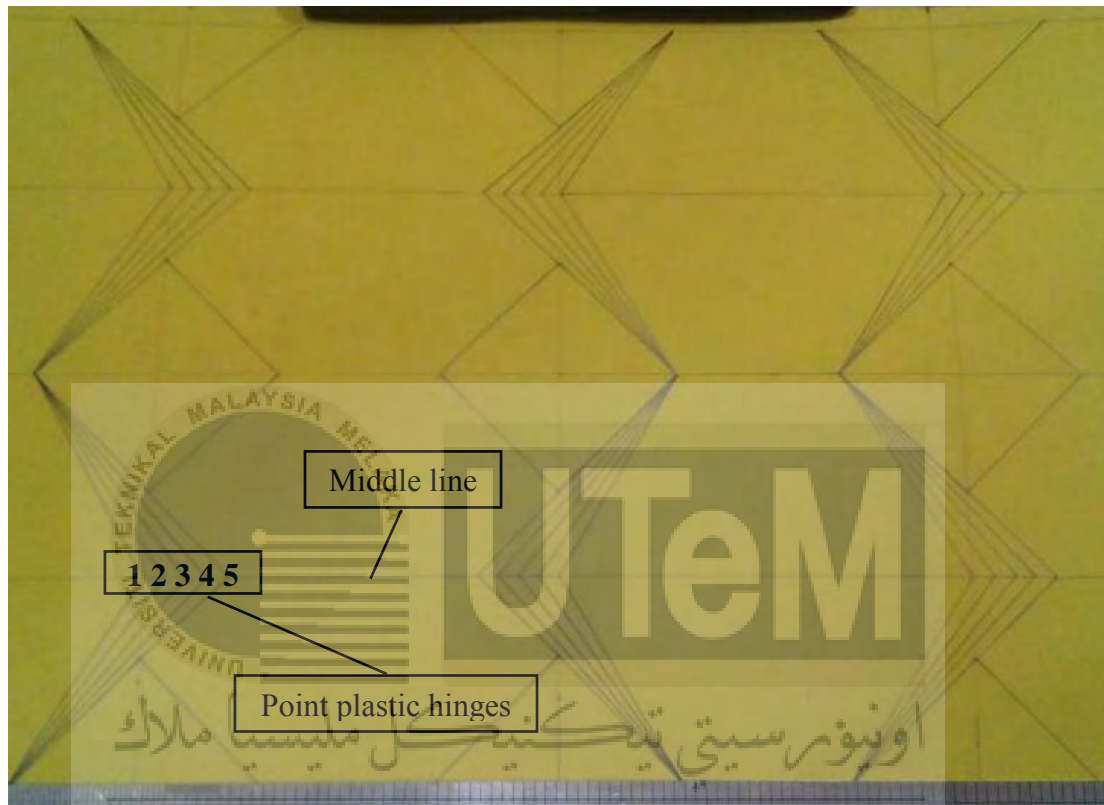


Figure 3. 21 : The lines of folding and point of plastic hinges

The distance between one points to another point of plastic hinges is 5mm. While, the total length of the plastic hinges from point 1 to point 5 is 20mm. The height and width of the one completed paper model is 100mm respectively.

## CHAPTER 4

### RESULTS AND ANALYSIS

#### 4.1 INTRODUCTION

This chapter discuss about the results obtained from the experimental work for all specimens. The theoretical results obtained from the previous studies will be discussed and compared with the results gained from the experimental work. Besides, the characteristics of the load displacement curve also will be discussed to explain the deforming modes for each tubes (aluminium and Poly vinyl chloride, PVC).

The paper model for square tubes only will be develop to show on how the deforming modes and movement of the plastic hinges occurred during compression events. The comparison between experimental results and theoretical results for plastic folding, mean load and energy absorbed will be analysed. The experimental work consists of two different materials which is aluminium and PVC tubes with three different in length for each tubes.

The objective of this chapter is to model the paper model of the deforming modes by using a thick paper in order it will be used as teaching tools. For this research, only the tensile and quasi static test were used to clarify the results.

## 4.2 TENSILE TEST

The purpose of this tensile test is to obtain the mechanical properties of the both materials which is aluminium and PVC. Figure 4.1 shown the results of tensile test specimens break for both material (aluminium and PVC). For aluminium tensile test specimen, it has very small deformation before failure because this aluminium are classified as brittle materials. Conversely, the different phenomena occurred on the PVC tensile test specimen which it has a large plastic deformation due to ductile materials compared to aluminium.



Figure 4. 1: Tensile test specimens break (aluminium and PVC)

### 4.2.1 GRAPH OF TENSILE STRESS AGAINST TENSILE STRAIN

Based on the Figure 4.2 and 4.3, it shows the sample graph obtained from the tensile test which tensile stress against tensile strain for aluminium and PVC tubes, respectively. As shown in Figure 4.2 and 4.3, at a yield point, the tensile test specimens is start to deform where the aluminium tensile test specimen will have small plastic deformation compared with PVC tensile test specimen due to brittleness properties. At the point of maximum load



indicated that the allowable load that the both materials able to withstand before failure. It clearly shown that aluminium material has a higher maximum load compared with PVC material due to their material properties.

Besides, at a break point, it shown that the tensile test specimen for both materials is undergoes failure because of increase in applied load or tension load on the tensile test specimens.

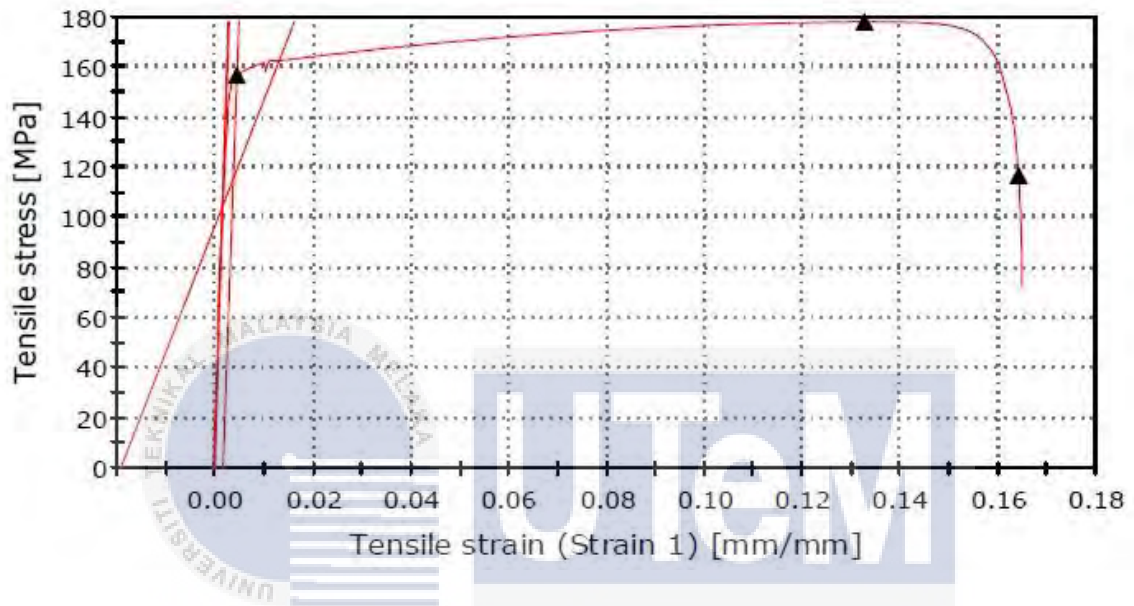


Figure 4. 2: Graph of tensile stress against tensile strain for aluminium

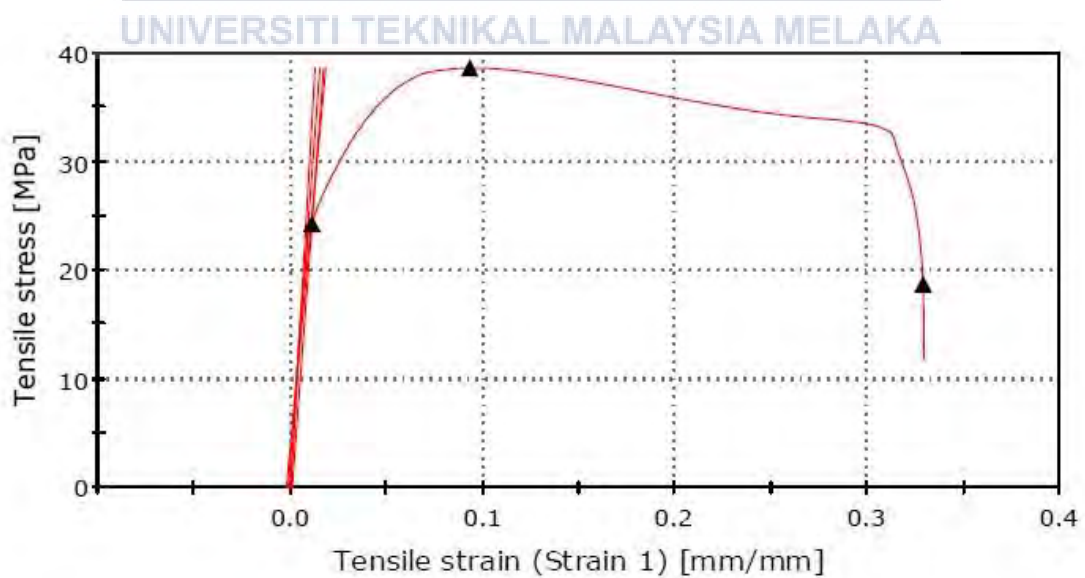


Figure 4. 3: Graph of tensile stress against tensile strain for PVC

#### 4.2.2 EXPERIMENTAL TENSILE TESTING RESULT

From the tensile testing, the results gained such as tensile stress at maximum load, tensile stress at yield, tensile strain at break and Young's modulus for aluminium and PVC materials are collected in the Table 4.1 and Table 4.2, respectively.

Table 4. 1: Experimental tensile testing result for aluminium

|                                      | Sample 1 | Sample 2 | Sample 3 | Average |
|--------------------------------------|----------|----------|----------|---------|
| Tensile stress at maximum load (MPa) | 177.976  | 182.644  | 180.240  | 180.287 |
| Tensile stress at yield (MPa)        | 156.837  | 161.519  | 158.888  | 159.081 |
| Tensile strain at break (mm/mm)      | 0.164    | 0.164    | 0.166    | 0.165   |
| Young's modulus (GPa)                | 65.480   | 61.500   | 59.647   | 62.209  |

Table 4. 2: Experimental tensile testing result for PVC

|                                      | Sample 1 | Sample 2 | Sample 3 | Average |
|--------------------------------------|----------|----------|----------|---------|
| Tensile stress at maximum load (MPa) | 38.592   | 38.299   | 37.472   | 38.121  |
| Tensile stress at yield (MPa)        | 24.285   | 24.373   | 23.769   | 24.142  |
| Tensile strain at break (mm/mm)      | 0.329    | 0.680    | 0.406    | 0.472   |
| Young's modulus (GPa)                | 3.036    | 3.016    | 2.912    | 2.988   |

The average tensile stress at yield for aluminium is 159.081 MPa is bigger than tensile stress at yield for PVC which is 24.142 MPa. It has a larger different due to high strength for aluminium materials compared with PVC materials. The value of Young's modulus for both materials is acceptable because this value is in a range of standard for each

materials. In general, based on the results obtained from tensile test, aluminium material has a higher strength compared with PVC material.

#### 4.3 TYPES OF DEFORMING MODES FOR ALUMINIUM AND PVC TUBES UNDER QUASI STATIC TEST

This quasi static test compress the aluminium and PVC tubes at very slow in speed which is 10mm/min. The rate of the testing speed will affected the types of the deforming modes. The quasi static test is the most suitable test to clarify the types of deforming modes of the tubes due to slow in testing speed. All of the tubes either aluminium or PVC tubes compressed only 60% from their total height.

##### 4.3.1 DEFORMING MODES FOR ALUMINIUM TUBES UNDER QUASI STATIC TEST

The types of deforming modes of the experimental work for square aluminium tubes indicated that all the three different in length of the tubes (100mm, 150mm and 200mm) deform in diamond mode. The thickness of this tubes is 1.3mm which is considered as moderate thickness that normally the tubes will deformed in the symmetrical mode as shown in Figure 4.4 and in Appendix C. If the tubes has very thin in wall thickness or thin tubes, it usually deformed in Euler or global buckling. This typical of tubes will affected the ability of energy absorption.

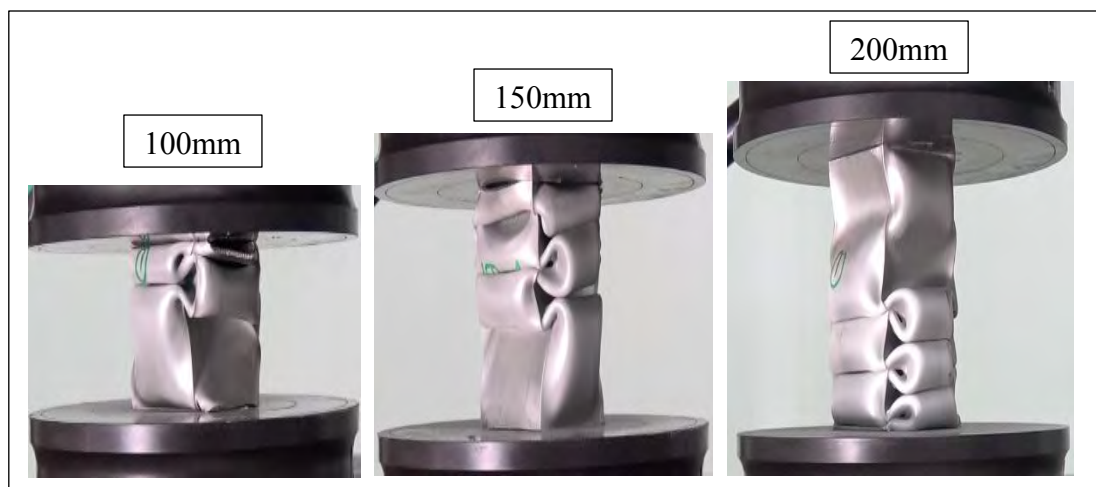


Figure 4. 4: Aluminium tubes with three different length (100mm, 150mm, 200mm)

The compression process of the square tubes in symmetrical mode indicated that the tubes deform progressively. Furthermore, the large plastic deformation concentrates on the middle part of folds and at the corner of the tubes. The rest of the area of the tubes will have very small plastic deformation. In addition, increase the length of the tubes will increase the number of folds.

For 100mm and 150mm tubes, the first folding occurred at the upper part of the tubes. Conversely, for the 200mm tubes, the tubes start to fold at the bottom part of the tubes. But, the same types of the deforming modes occurred on all of the three tubes which is diamond modes either it start to fold at upper or bottom part of the tubes. The time taken for the tubes to compressed 60% from their total length is collected in the Table 4.3. It can be seen that the directly proportional relationship between length of the tubes and time taken to compress 60% of the total length.

Table 4. 3: Time taken for the tubes to compressed 60% from their total length

| Tubes | Height (mm) | Time taken to compress 60% of total length (minutes) |
|-------|-------------|--|
| 1     | 100         | ± 6  |
| 2     | 150         | ± 9  |
| 3     | 200         | ± 12   |

### 4.3.2 DEFORMING MODES FOR PVC TUBES UNDER QUASI STATIC TEST

For the circular PVC tube, the types of deforming modes is depending on the radius/thickness ( $r/t$ ) ratio of the tubes. If the ratio  $r/t < 15$ , the tubes will deformed in concertina mode. Conversely, if the ratio  $r/t > 15$ , the tubes will deformed in diamond modes. The possibility of this circular PVC tubes is will compressed in 3 types of deforming modes which is concertina modes, diamond modes and mixture modes. Results from the experimental work shows that all the three different in length of the tubes (100mm, 150mm and 200mm) deform in diamond mode as shown in Figure 4.5 and in Appendix D.

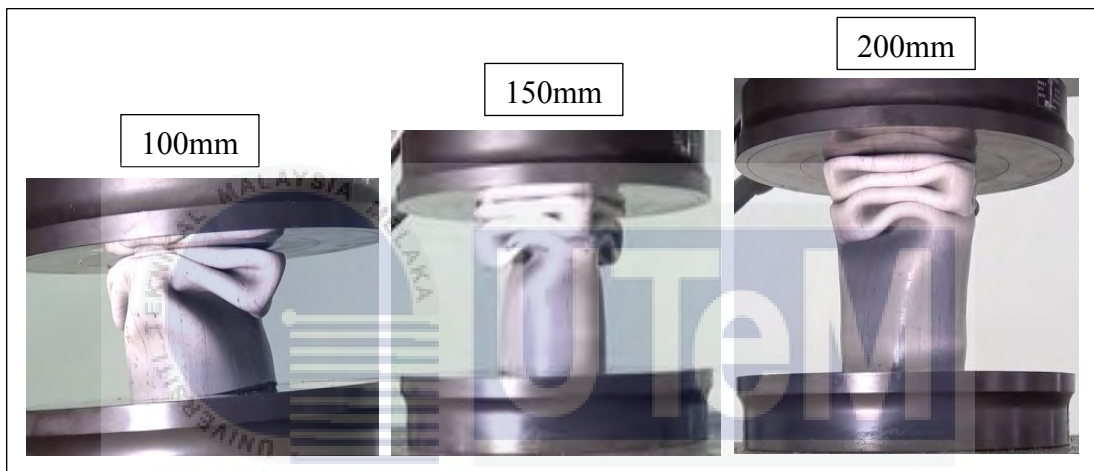


Figure 4. 5: PVC tubes with three different length (100mm, 150mm, 200mm)

UNIVERSITI TEKNIKAL MALAYSIA MELAKA

Based on the Figure 4.5, the compression process of the circular PVC tube deform progressively along the length of the tubes. In addition, the large plastic deformation occurred especially along the circumference of the tubes. Small plastic deformation also occurred at a middle part of folds. The phenomenon of large plastic deformation is due to ductility of the tubes. PVC tubes in characterise as non-metallic materials where has larger plastic deformation as a results of compression or tension process. The same behaviour occurred as aluminium tubes where the increase the length of the tubes will increase the number of folds.

For all three different length of the tubes, the first folding occurred at the upper part of the tubes and deform progressively one by one until it compress for only 60 % of their total length. The time taken for the tubes to compressed 60% from their total length is same as aluminium tubes as shown in the Table 4.3.

#### 4.4 QUASI STATIC TEST RESULT

The main objective carried out the quasi static test is to obtain the type of the deforming modes of the tubes in purpose of modelling using thick paper. There are two type of tubes has been selected which is square aluminium tube and circular polyvinyl chloride, PVC tubes. There are three sample for each length of the tubes will be tested under this test. The series of deforming modes of the tubes is recorded to shows the compression phenomenon of this test. Besides, the results such as maximum load, compressive stress and extension at maximum load, total area under the curve, mean load and plastic folding are obtained from this testing. This results also will be compared with theoretical value.

##### 4.4.1 SQUARE ALUMINIUM TUBE WITH LENGTH 100mm

For square aluminium tube with (length,  $L=100\text{mm}$ , thickness,  $t=1.3\text{mm}$ , width,  $w = 44.5\text{mm}$ ), are deformed in diamond mode for all three sample. Figure 4.6 shows the load displacement curve for sample 1 obtained from the testing. Every peak on the graph is represents the resulted of fold for square aluminium. The graph shows a three highest peaks, means that the tube produce there folds. The series picture of progressive deforming mode of the tube for sample 1 are shown in Figure 4.7.

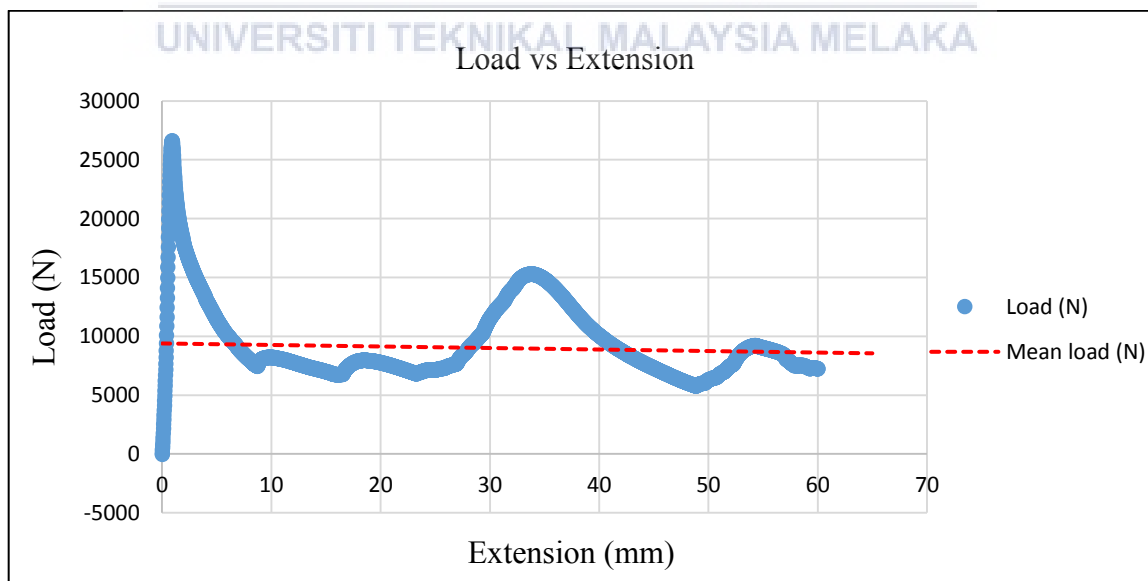


Figure 4. 6: Sample 1 of load displacement curve for the aluminium tube with length 100mm

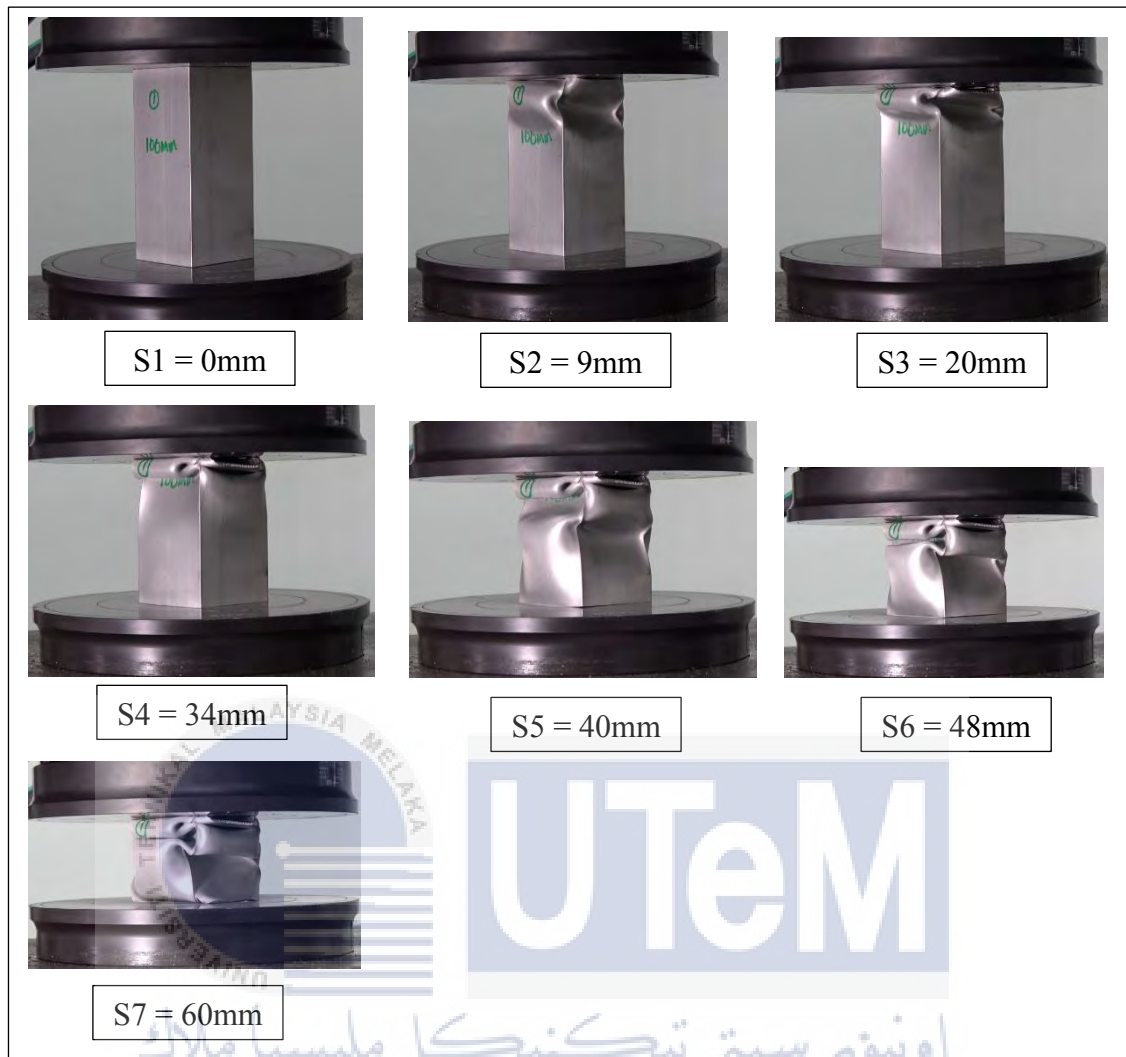


Figure 4. 7: Sample 1 of deforming mode for aluminium tube with length 100mm

Based on Figure 4.6, the first peak which is maximum load or  $P_{peak}$  where the tube is started to fold at deformation of 0.92mm. The value of  $P_{peak}$  for this sample is 26.62 kN. The load is decreased to 7.2 kN at 9mm it deformed as shown at picture S2. Then, this load increase for the second highest peak which is 16.2 kN at deformation of 34mm as shown at picture S4. At this point, this tube started to produce a second fold. After that, the load is drop back to 5.1 kN at deformation of 48mm as shown at picture S6. For this point, the tube already produced 2 folds. Next, the load increase again until reached a point 9.8 kN as a starting point to produce a third fold at deformation of 55mm.

Lastly, the load decreased again until 7.2 kN at deformation of 60mm as shown at picture S7. At this point, the tube produced the third fold but not as a completed fold. The testing stop at that point because already reached the point of 60% from the total length of

the tube which is 60mm. As a conclusion, sample 1 has produced up to three folds. Every time this tube started to produce a fold, the load will increased and dropped back when the fold is completely produced.

#### **4.4.1.1 COMPARISON BETWEEN EXPERIMENTAL AND THEORETICAL VALUE FOR ALUMINIUM TUBE WITH LENGTH 100mm**

Table 4.4 shows the results is tabulated for experimental and theoretical value for square aluminium tube with length 100mm. The percentage of error for energy absorbed, mean load and plastic folding are calculated. From theoretical studies conducted by Singace, the percentage error for energy absorbed for sample 1, sample 2 and sample 3 are 12.64%, 3.98% and 14.77% respectively. According to this results, the difference between experimental and theoretical results is not too large. Means that, the progressive deformation for all three sample produced a close results of energy absorbed between experimental and theoretical value.

Besides, for the mean load, the percentage of error for sample 1, sample 2 and sample 3 are 12.6%, 3.95% and 14.8% respectively. According to Singace theorem, the mean load is depends on the energy absorbed because deformation for this testing is constant which is 60mm. The relationship between energy absorbed and mean load is directly proportional. So, if the error for energy absorbed increased, the error for mean load also will be increased.

Next, the percentage of error for plastic folding shows very close error. For sample 1, sample 2 and sample 3, the error that has been calculated using Singace theorem are 5.16%, 2.08% and 1.45% respectively. The close result of error is due to progressive deformation for all three tubes. The length of the plastic folding almost same for every fold. So, based on theoretically, the total of fold that should happened is around 2 or 3 folds.



Table 4. 4: Comparison between experimental and theoretical results of quasi-static testing for aluminium tube with length 100mm

| Sample   | Max load (kN) | Compression stress at max load (MPa) | Compressive extension at max load (mm) | Experimental               |                      |                           | Theoretical                |                      |            |            |            |      |
|----------|---------------|--------------------------------------|--|----------------------------|----------------------|---------------------------|----------------------------|----------------------|------------|------------|------------|------|
|          |               |                                      |  | Total area under graph (J) | Mean load, $P_m$ (N) | Plastic folding, 2Hm (mm) | Total area under graph (J) | Mean load, $P_m$ (N) | % of error | % of error | % of error |      |
| Sample 1 | 26.62         | 150.86                               | 0.92                                   | 564.02                     | 9398.22              | 28.33                     | 500.71                     | 8345.12              | 12.64      | 12.60      | 26.94      | 5.16 |
| Sample 2 | 28.13         | 159.44                               | 0.65                                   | 520.65                     | 8674.56              | 27.50                     | 500.71                     | 8345.12              | 3.98       | 3.95       | 26.94      | 2.08 |
| Sample 3 | 26.58         | 150.64                               | 0.53                                   | 426.77                     | 7109.19              | 27.33                     | 500.71                     | 8345.12              | 14.77      | 14.8       | 26.94      | 1.45 |

#### 4.4.2 SQUARE ALUMINIUM TUBE WITH LENGTH 150mm

For square aluminium tube with same thickness and width but different in length which is 150mm are deformed in diamond mode for all three sample. Figure 4.8 shows the load displacement curve for sample 3 obtained from the experimental. Every peak on the graph is represents the resulted to form a fold for square aluminium. The graph shows a four highest peaks, means that the tube produce four folds. The series picture of progressive deforming mode of the tube for sample 3 are shown in Figure 4.9.

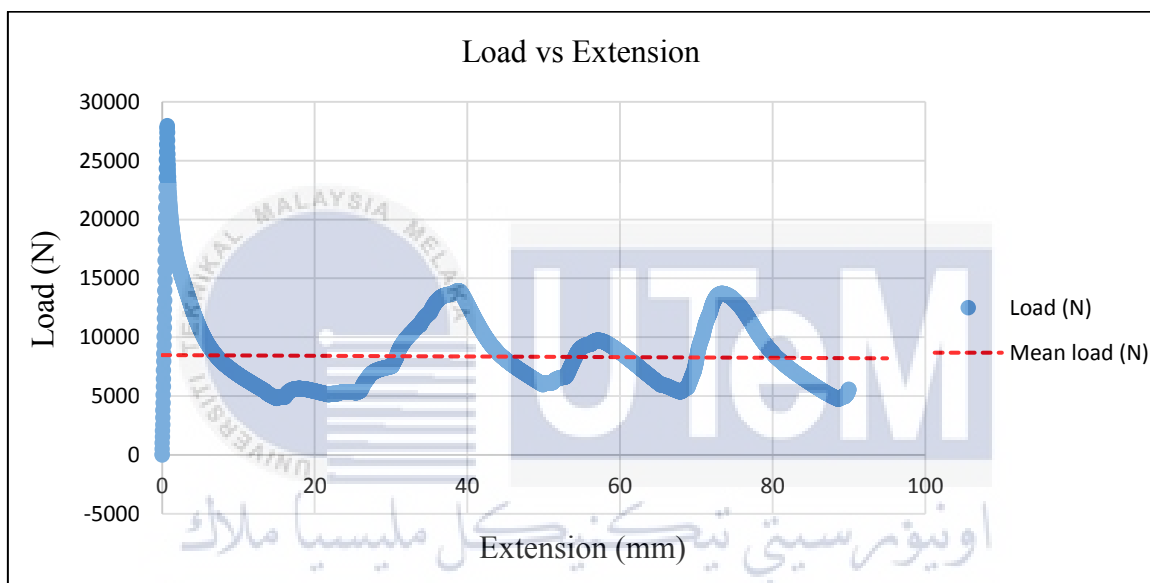


Figure 4. 8: Sample 3 of load displacement curve for the aluminium tube with length 150mm

Based on Figure 4.8, the first peak which is maximum load or  $P_{peak}$  where the tube is started to fold at deformation of 0.68mm. The value of  $P_{peak}$  for this sample is 27.98 kN. The load is decreased to 4.8 kN at 14mm it deformed as shown at picture S2. Then, this load increase for the second highest peak which is 14.8 kN at deformation of 38mm as shown at picture S4. At this point, this tube started to produce a second fold. After that, the load is drop back to 5.9 kN at deformation of 50mm as shown at picture S6. For this point, the tube already produced 2 folds. Next, the load increase again until reached a point 10 kN as a starting point to produce a third fold at deformation of 57mm. Then, the load decreased again until 5 kN at deformation of 68mm as shown at picture S7. At this point, the tube has produced three completed fold. The load continued to increase until reached 9.5 kN at

deformation of 75mm as shown at picture S8. Lastly, the load drop until 4.8 kN at deformation of 88mm as shown at picture S9. The testing stop at point S10 because already reached the point of 60% from the total length of the tube which is 90mm. As a conclusion, the progressive deformation of sample 3 has produced up to 4 completed folds.

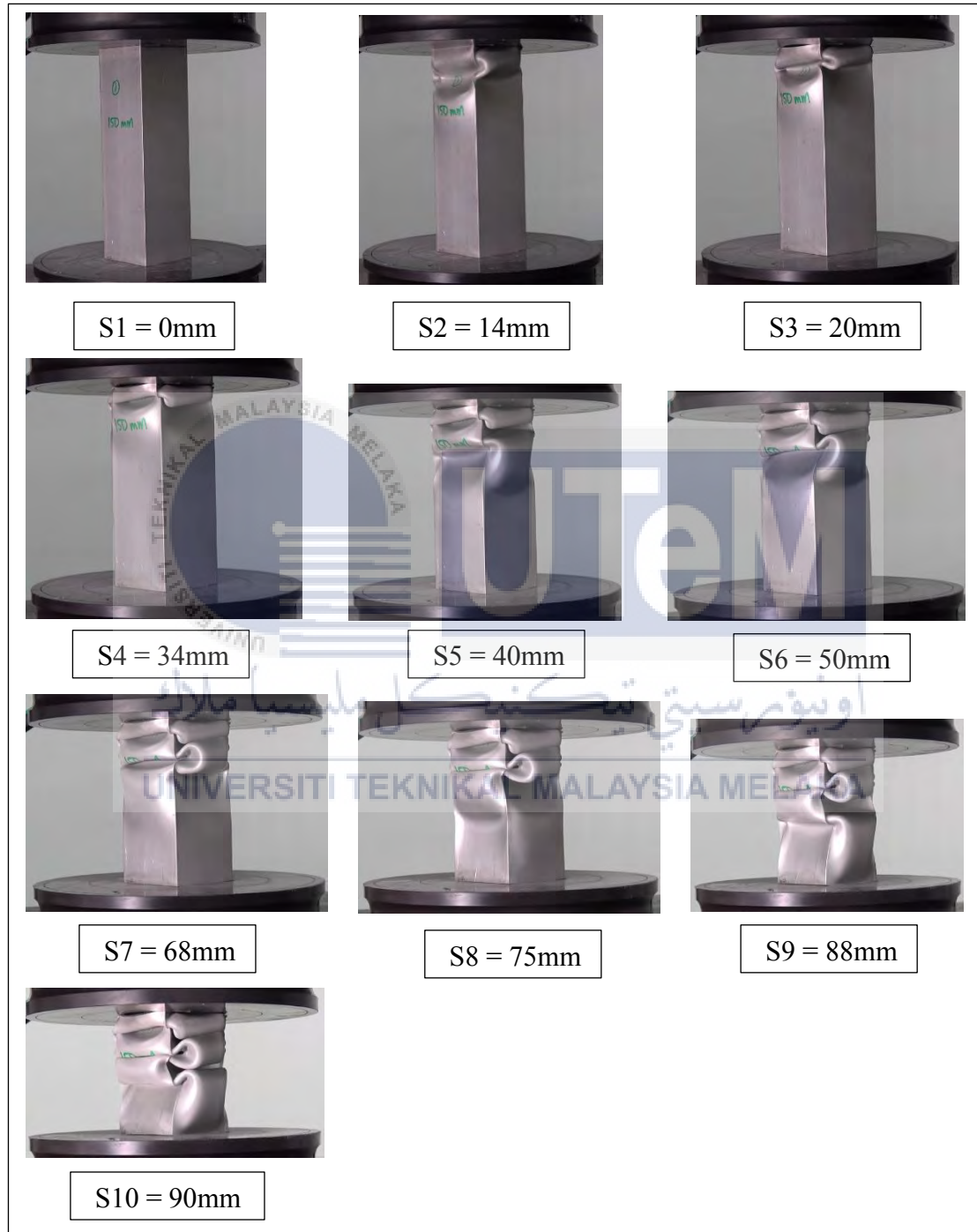


Figure 4. 9: Sample 1 of deforming mode for aluminium tube with length 150mm

#### 4.4.2.1 COMPARISON BETWEEN EXPERIMENTAL AND THEORETICAL VALUE FOR ALUMINIUM TUBE WITH LENGTH 150mm

Table 4.5 shows the results is tabulated for experimental and theoretical value for square aluminium tube with length 150mm. The percentage of error for energy absorbed, mean load and plastic folding are calculated. From theoretical studies conducted by Singace, the percentage error for energy absorbed for sample 1, sample 2 and sample 3 are 19.04%, 12.09% and 1.63% respectively. According to this results, the difference between experimental and theoretical results is not too large except for sample 1. Means that, the progressive deformation for all three sample produced a close results of energy absorbed between experimental and theoretical value.

Besides, for the mean load, the percentage of error for sample 1, sample 2 and sample 3 are 19.10%, 12.10% and 1.62% respectively. According to Singace theorem, the mean load is depends on the energy absorbed because deformation for this testing is constant which is 90mm. The relationship between energy absorbed and mean load is directly proportional. So, if the error for energy absorbed increased, the error for mean load also will be increased. It clearly can be seen that the percentage of error of mean load for sample 1 is highest due to highest of percentage of error for energy absorbed.

Next, the percentage of error for plastic folding shows not too large for all three sample. For sample 1, sample 2 and sample 3, the error that has been calculated using Singace theorem are 10.43%, 9.99% and 12.29% respectively. The error is due to not completely compress through the total length of the tube. If the tubes is compress completely and produced progressive deformation, the plastic folding will be same for each fold and also for all samples. The length of the plastic folding almost same for every fold either inward or outward folding for this experimental work. So, based on theoretically, the total of fold that should happened is around 4 or 5 folds.

Table 4. 5: Comparison between experimental and theoretical results of quasi-static testing for aluminium tube with length 150mm

| Sample   | Max load (kN) | Compression stress at max load (MPa) | Compressive extension at max load (mm) | Experimental               |                      |                              | Theoretical                |                      |            |                       |            |
|----------|---------------|--------------------------------------|--|----------------------------|----------------------|------------------------------|----------------------------|----------------------|------------|-----------------------|------------|
|          |               |                                      |  | Total area under graph (J) | Mean load, $P_m$ (N) | Plastic folding, $2H_m$ (mm) | Total area under graph (J) | Mean load, $P_m$ (N) | % of error | Plastic folding, (mm) | % of error |
| Sample 1 | 26.86         | 152.22                               | 0.60                                   | 608.06                     | 6754.79              | 29.75                        | 751.06                     | 8345.12              | 19.10      | 26.94                 | 10.43      |
| Sample 2 | 29.50         | 167.21                               | 0.75                                   | 841.90                     | 9353.78              | 29.63                        | 751.06                     | 8345.12              | 12.10      | 26.94                 | 9.99       |
| Sample 3 | 27.98         | 158.56                               | 0.68                                   | 763.29                     | 8480.06              | 30.25                        | 751.06                     | 8345.12              | 1.62       | 26.94                 | 12.29      |

#### 4.4.3 SQUARE ALUMINIUM TUBE WITH LENGTH 200mm

For square aluminium tube also with same thickness and width but different in length which is 200mm are deformed in diamond mode for all three sample. Figure 4.10 shows the load displacement curve for sample 1 obtained from the experimental. Every peak on the graph is represents the resulted to form a fold for square aluminium. There are six highest peaks shown on this graph, means that the tube will produced six folds. This sample of tube with 200mm in length start to fold from bottom part of the tube followed one by one until produced about six folds. It looks different from the tube with length 100mm and 150mm where started to fold from upper part of the tubes. But, there are no different in deforming modes for all three different length either started to fold from upper or bottom part of the tubes which are produced a diamond modes. The series picture of progressive deforming mode of the tube for sample 1 are shown in Figure 4.11.

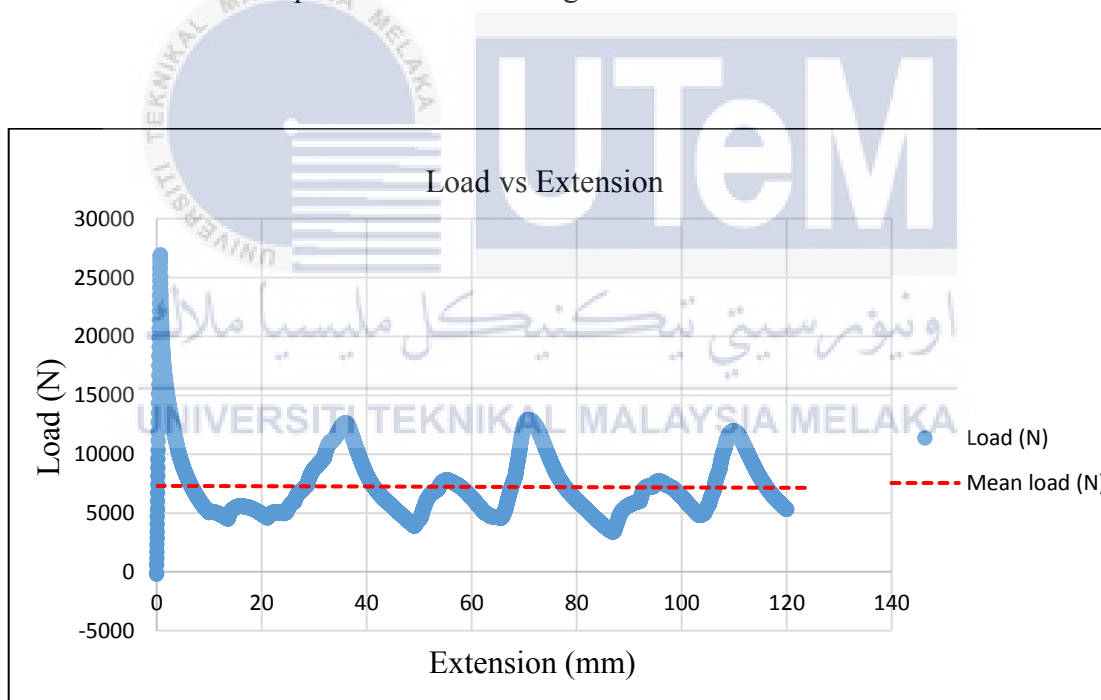


Figure 4. 10: Sample 1 of load displacement curve for the aluminium tube with length 200mm

Based on Figure 4.10, the first peak which is maximum load or  $P_{\text{peak}}$  where the tube is started to fold at deformation of 0.80mm. The value of  $P_{\text{peak}}$  for this sample is 28.41 kN. The load is decreased to 4.5 kN at 13mm it deformed as shown at picture S1.

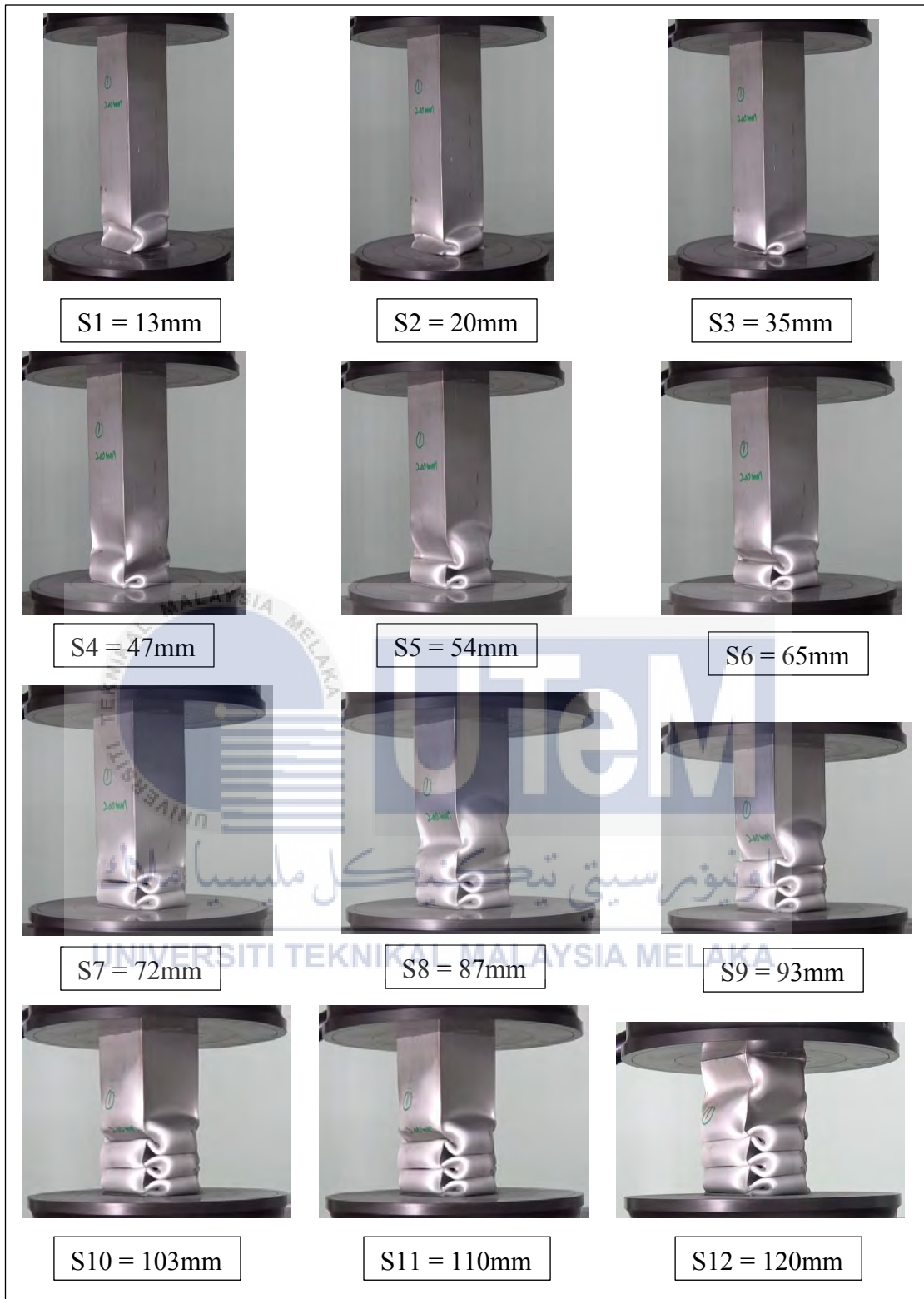


Figure 4. 11: Sample 1 of deforming mode for aluminium tube with length 200mm

Then, this load increase for the second highest peak which is 13.7 kN at deformation of 35mm as shown at picture S3. At this point, this tube started to produce a second fold.

After that, the load is drop back to 4.1 kN at deformation of 47mm as shown at picture S4. For this point, the tube already produced 2 folds. Next, the load increase again until reached a point 8.2 kN as a starting point to produce a third fold at deformation of 54mm. Then, the load dropped again until 4.5 kN at deformation of 65mm as shown at picture S6. At this point, the tube has produced three completed fold. The load continued to increase drastically until reached 14.1 kN at deformation of 72mm as shown at picture S7.

Next, the load dropped again until 3.7 kN at deformation of 87mm as shown at picture S8. The tubes already produced a completed four folds. The testing is continued again until the load increased to 8.6 kN at deformation of 93mm as shown at picture S9. Same phenomenon occurred where the load is decreased due to producing a fold until a point of 4.8 kN at deformation 103mm as shown at picture S10. In producing an into six fold, the load is increased again until 13.1 kN at deformation 110mm as shown at picture S11 and dropped again until 5 kN to produce a completed six folds.

The testing stop at point S12 because already reached the point of 60% from the total length of the tube which is 120mm. As a conclusion, the progressive deformation of sample 1 for aluminium tube with length 200mm has produced up to 6 completed folds.



#### **4.4.3.1 COMPARISON BETWEEN EXPERIMENTAL AND THEORETICAL VALUE FOR ALUMINIUM TUBE WITH LENGTH 200mm**

Table 4.6 shows the results is tabulated for experimental and theoretical value for square aluminium tube with length 200mm. The percentage of error for energy absorbed, mean load and plastic folding are calculated. From theoretical studies conducted by Singace, the percentage error for energy absorbed for sample 1, sample 2 and sample 3 are 1.69%, 9.30% and 12.46% respectively. According to this results, the difference between experimental and theoretical results is not too large for all three samples. Means that, the progressive deformation for all three sample produced a close results of energy absorbed between experimental and theoretical value.

Besides, for the mean load, the percentage of error for sample 1, sample 2 and sample 3 are 1.69%, 9.32% and 12.50% respectively. According to Singace theorem, the mean load is depends on the energy absorbed because deformation for this testing is constant which is 120mm. The relationship between energy absorbed and mean load is directly proportional. So, if the error for energy absorbed increased, the error for mean load also will be increased. It clearly can be seen that the percentage of error of mean load for sample 1 is lowest due to lowest of percentage of error for energy absorbed.

Next, the percentage of error for plastic folding shows a quite large for all three sample. For sample 1, sample 2 and sample 3, the error that has been calculated using Singace theorem are 14.33%, 13.21% and 15.07% respectively. The error is due to not completely compress through the total length of the tube. If the tubes is compress completely and produced progressive deformation, the plastic folding will be same for each fold and also for all samples. The length of the plastic folding almost same for every fold either inward or outward folding for this experimental work. So, based on theoretically, the total of fold that should happened is around 6 or 7 folds. Increased in length of compression process will increased the number of folds.

Table 4. 6: Comparison between experimental and theoretical results of quasi-static testing for aluminium tube with length 200mm

| Sample   | Max load (kN) | Compression stress at max load (MPa) | Compressive extension at max load (mm) | Experimental               |                      |                              | Theoretical                |                      |            |                       |            |
|----------|---------------|--------------------------------------|--|----------------------------|----------------------|------------------------------|----------------------------|----------------------|------------|-----------------------|------------|
|          |               |                                      |  | Total area under graph (J) | Mean load, $P_m$ (N) | Plastic folding, $2H_m$ (mm) | Total area under graph (J) | Mean load, $P_m$ (N) | % of error | Plastic folding, (mm) | % of error |
| Sample 1 | 28.41         | 161.04                               | 0.80                                   | 1018.34                    | 8486.38              | 30.8                         | 1001.41                    | 8345.12              | 1.69       | 26.94                 | 14.33      |
| Sample 2 | 27.17         | 154.01                               | 0.72                                   | 908.25                     | 7567.51              | 30.5                         | 1001.41                    | 8345.12              | 9.30       | 26.94                 | 13.21      |
| Sample 3 | 26.94         | 152.72                               | 0.70                                   | 876.61                     | 7304.17              | 31.0                         | 1001.41                    | 8345.12              | 12.46      | 26.94                 | 15.07      |

#### 4.4.4 SAMPLE CALCULATION FOR SQUARE ALUMINIUM TUBES

The energy absorbed, mean load and plastic folding is calculated using Singace theorem. The value of tensile stress at yield, width and thickness of tubes are tabulated in Table 4.7. The value of tensile stress at yield is gained from tensile test.

Table 4. 7: Properties of square aluminium tubes

| Tensile stress at yield, $\sigma_u$<br>(MPa) | Width of tube, w<br>(mm) | Thickness of tube, t<br>(mm) |
|--|--------------------------|------------------------------|
| 159.08                                       | 44.5                     | 1.3                          |

From the previous studies, the equation given are :

For mean load,  $P_m$  :

$$P_m = 9.56 \sigma_u \sqrt[3]{wt^5} \quad (4.1)$$

$$P_m = 9.56 (159.08 \times 10^6) \sqrt[3]{(0.0445)(0.0013)^5}$$

$$P_m = 8345.12 \text{ N}$$

For half plastic folding,  $H_m$  :

$$H_m = 0.983 \sqrt[3]{w^2 t} \quad (4.2)$$

$$H_m = 0.983 \sqrt[3]{(0.0445)^2 (0.0013)}$$

$$H_m = 13.47 \text{ mm}$$

So, for one completed plastic folding is,  $2H_m = 26.94 \text{ mm}$

For energy absorbed :

$$E = P_m \times \text{deformation, } S \quad (4.3)$$

1) For 100mm length of tube, deformation,  $S = 60\text{mm}$

$$E = 8345.12 \times 0.06$$

$$E = 500.71 \text{ J}$$

2) For 150mm length of tube, deformation,  $S = 90\text{mm}$

$$E = 8345.12 \times 0.09$$

$$E = 751.06 \text{ J}$$

3) For 200mm length of tube, deformation,  $S = 120\text{mm}$

$$E = 8345.12 \times 0.12$$

$$E = 1001.41 \text{ J}$$

For percentage of error, % :

$$\% \text{ error} = \frac{\text{experimental value} - \text{theoretical value}}{\text{theoretical value}} \times 100\% \quad (4.4)$$

Example calculation for percentage of error for mean load, energy absorbed and plastic folding for 100mm length of tube (sample 1) are shown below, respectively.

$$1) \% \text{ error} = \frac{9398.22 - 8345.12}{8345.12} \times 100\%$$

$$\% \text{ error} = 12.62 \%$$

$$2) \% \text{ error} = \frac{564.02 - 500.71}{500.71} \times 100\%$$

$$\% \text{ error} = 12.64 \%$$

$$3) \% \text{ error} = \frac{28.33 - 26.94}{26.94} \times 100\%$$

$$\% \text{ error} = 5.16 \%$$

#### 4.4.5 CIRCULAR PVC TUBE WITH LENGTH 100mm

For circular PVC tube with (length,  $L=100\text{mm}$ , thickness,  $t=2.9\text{mm}$ , outer diameter,  $d = 60.2\text{mm}$ ), are deformed in diamond mode for all three sample. Figure 4.12 shows the load displacement curve for sample 1 obtained from the testing. Every peak on the graph is represents the resulted of fold for circular PVC tube. The graph shows a three highest peaks, means that the tube produce there folds. The series picture of progressive deforming mode of the tube for sample 1 are shown in Figure 4.13.

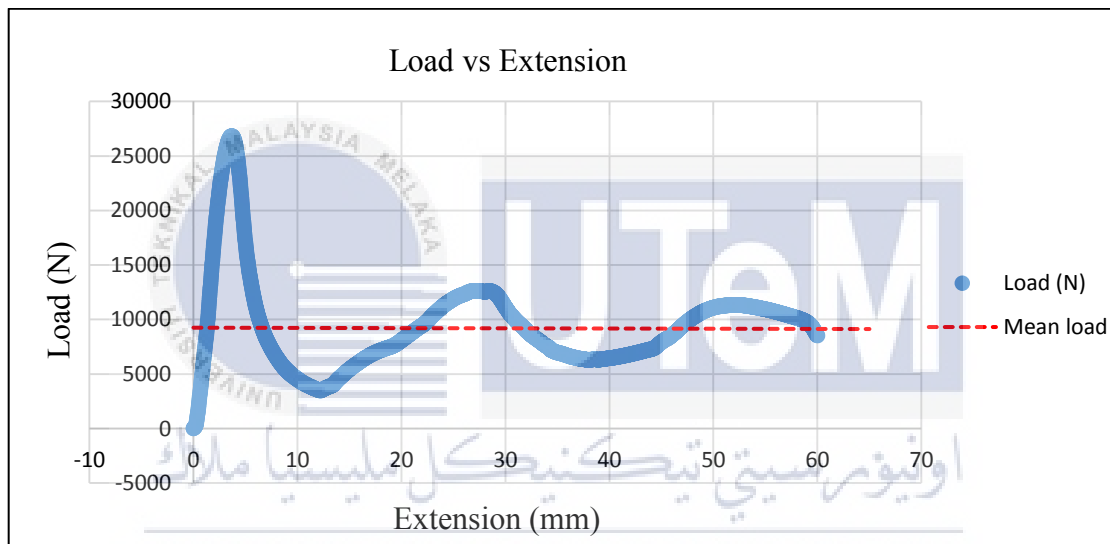


Figure 4. 12: Sample 1 of load displacement curve for PVC tube with length 100mm

Based on Figure 4.12, the first peak which is maximum load or  $P_{\text{peak}}$  where the tube is started to fold at deformation of 3.81mm. The value of  $P_{\text{peak}}$  for this sample is 27.95 kN. The load is decreased drastically to 3.2 kN at 12mm it deformed as shown at picture S2. Then, this load increase for the second highest peak which is 13.1 kN at deformation of 28mm as shown at picture S4. At this point, this tube started to produce a second fold. After that, the load is drop back to 5.9 kN at deformation of 39mm as shown at picture S5. For this point, the tube already produced 2 folds. Next, the load increase again until reached a point 12.3 kN as a starting point to produce a third fold at deformation of 52mm.

Lastly, the load decreased again until 8.9 kN at deformation of 60mm as shown at picture S7. At this point, the tube produced the third fold but not as a completed fold. The testing stop at that point because already reached the point of 60% from the total length of the tube which is 60mm. As a conclusion, sample 1 has produced up to three folds. Every time this tube started to produce a fold, the load will increased and dropped back when the fold is completely produced.

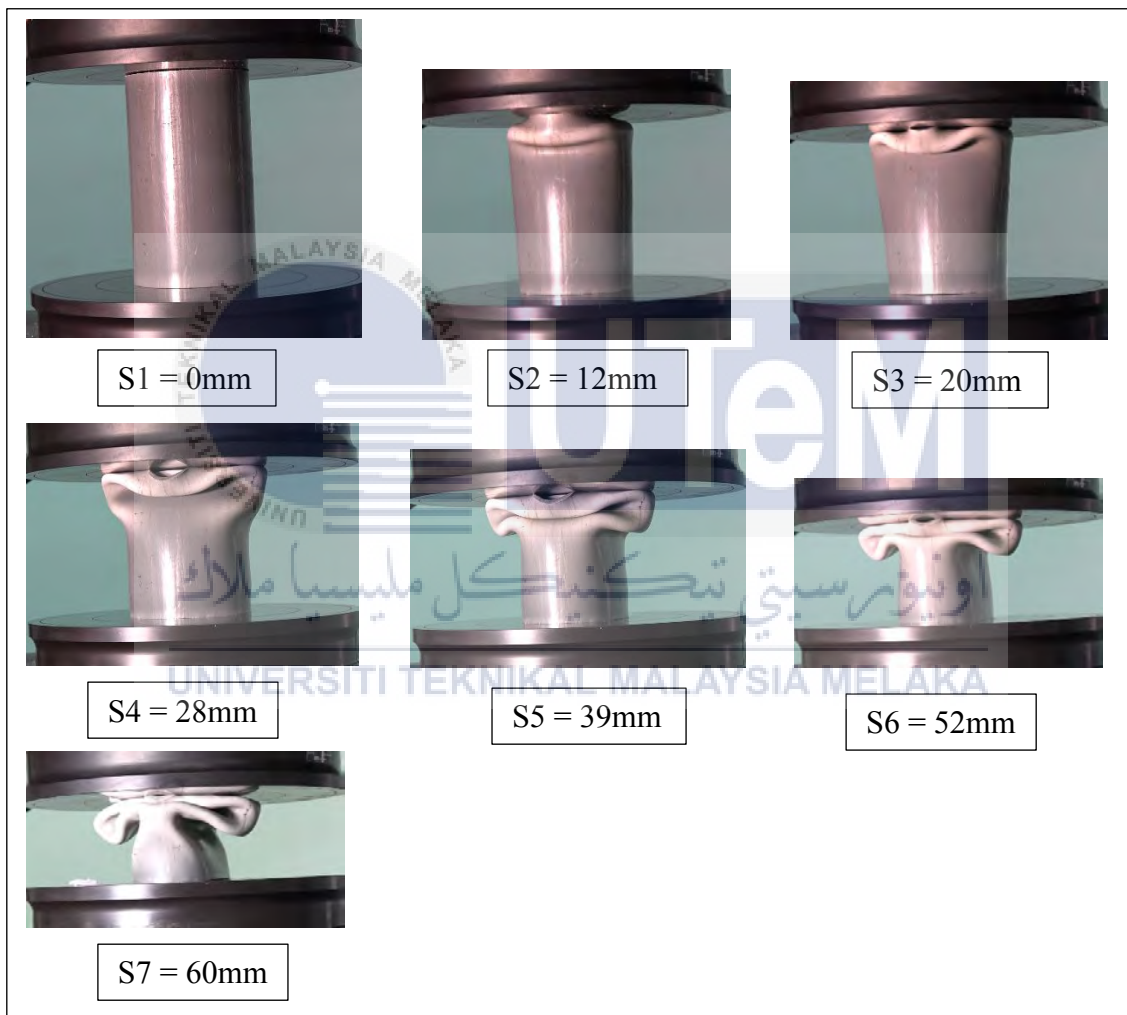


Figure 4. 13: Sample 1 of deforming mode for PVC tube with length 100mm

#### **4.4.5.1 COMPARISON BETWEEN EXPERIMENTAL AND THEORETICAL VALUE FOR PVC TUBE WITH LENGTH 100mm**

Table 4.8 shows the results is tabulated for experimental and theoretical value for circular PVC tube with length 100mm. The percentage of error for energy absorbed, mean load and plastic folding are calculated. From theoretical studies conducted by Singace, the percentage error for energy absorbed for sample 1, sample 2 and sample 3 are 23.00%, 19.80% and 19.20% respectively. According to this results, the difference between experimental and theoretical results is quite large. Means that, the progressive deformation for all three sample produced a quite large different for energy absorbed between experimental and theoretical value due to highest plastic deformation of the tubes (ductility).

Besides, for the mean load, the percentage of error for sample 1, sample 2 and sample 3 are 23.10%, 22.20% and 19.20% respectively. The result shows a quite large of different between experimental and theoretical value. According to Singace theorem, the mean load is depends on the energy absorbed because deformation for this testing is constant which is 60mm. The relationship between energy absorbed and mean load is directly proportional. So, if the error for energy absorbed increased, the error for mean load also will be increased.

Next, the percentage of error for plastic folding shows very close error. For sample 1, sample 2 and sample 3, the error that has been calculated using Singace theorem are 6.37%, 4.38% and 3.98% respectively. The close result of error is due to progressive deformation for all three tubes. So, based on theoretically, the total of fold that should happened is around 2 or 3 folds.

Table 4. 8: Comparison between experimental and theoretical results of quasi-static testing for PVC tube with length 100mm

| Sample   | Max load (kN) | Compression stress at max load (MPa) | Compressive extension at max load (mm) | Experimental               |                      |                              | Theoretical                |            |                       |            |                       |            |
|----------|---------------|--------------------------------------|--|----------------------------|----------------------|------------------------------|----------------------------|------------|-----------------------|------------|-----------------------|------------|
|          |               |                                      |  | Total area under graph (J) | Mean load, $P_m$ (N) | Plastic folding, $2H_m$ (mm) | Total area under graph (J) | % of error | Mean load, $P_m$ (kN) | % of error | Plastic folding, (mm) | % of error |
| Sample 1 | 27.95         | 54.24                                | 3.81                                   | 548.79                     | 9143.32              | 23.50                        | 713.10                     | 23.00      | 11.89                 | 23.10      | 25.10                 | 6.37       |
| Sample 2 | 26.83         | 52.06                                | 3.68                                   | 571.58                     | 9250.33              | 24.00                        | 713.10                     | 19.80      | 11.89                 | 22.20      | 25.10                 | 4.38       |
| Sample 3 | 27.75         | 53.86                                | 3.38                                   | 576.41                     | 9601.82              | 24.10                        | 713.10                     | 19.20      | 11.89                 | 19.20      | 25.10                 | 3.98       |



#### 4.4.6 CIRCULAR PVC TUBE WITH LENGTH 150mm

For circular PVC tube with same thickness and outer diameter but different in length which is 150mm are deformed in diamond mode for all three sample. Figure 4.14 shows the load displacement curve for sample 1 obtained from the experimental work. Every peak on the graph is represents the resulted to form a fold for circular PVC. The graph shows a four highest peaks, means that the tube produce four folds. The series picture of progressive deforming mode of the tube for sample 1 are shown in Figure 4.15.

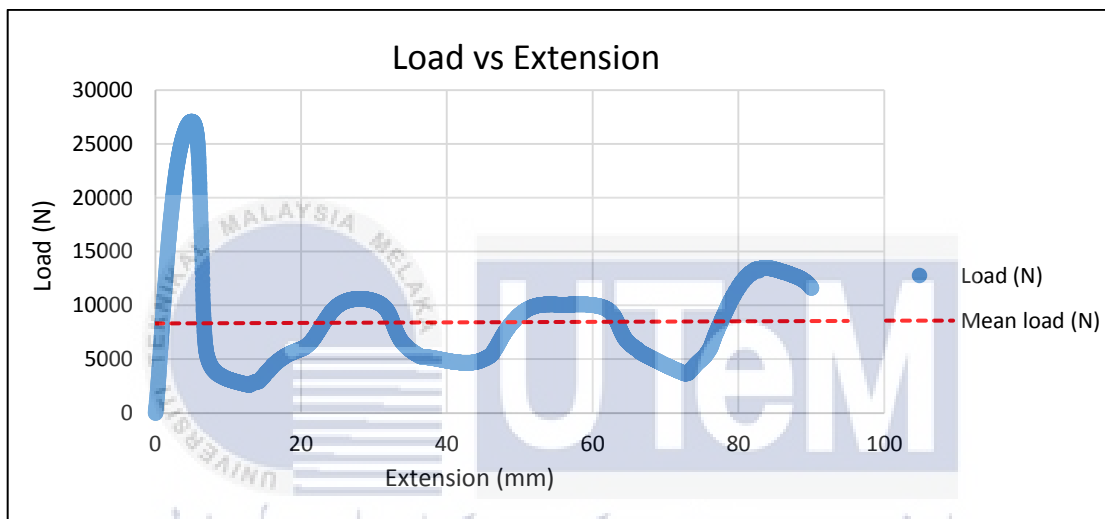


Figure 4. 14: Sample 1 of load displacement curve for PVC tube with length 150mm

Based on Figure 4.14, the first peak which is maximum load or  $P_{\text{peak}}$  where the tube is started to fold at deformation of 4.96mm. The value of  $P_{\text{peak}}$  for this sample is 27.09 kN. The load decreased drastically to 2.5 kN at 12mm it deformed as shown at picture S2. Then, this load increase for the second highest peak which is 10.8 kN at deformation of 27mm as shown at picture S4. At this point, this tube started to produce a second fold. After that, the load is drop back to 4.5 kN at deformation of 40mm as shown at picture S5. For this point, the tube already produced 2 folds. Next, the load increase again until reached a point 10.2 kN as a starting point to produce a third fold at deformation of 52mm. Then, the load decreased again until 3.9 kN at deformation of 72mm as shown at picture S8. At this point, the tube has produced three completed fold. The load continued to increase until reached 14.5 kN at deformation of 82mm as shown at picture S9.

Lastly, the load drop until 10.9 kN at deformation of 90mm as shown at picture S10. The testing stop at that point because already reached the point of 60% from the total length of the tube which is 90mm. As a conclusion, the progressive deformation of sample 1 has produced up to 4 completed folds.



Figure 4. 15: Sample 1 of deforming mode for PVC tube with length 150mm

#### 4.4.6.1 COMPARISON BETWEEN EXPERIMENTAL AND THEORETICAL VALUE FOR PVC TUBE WITH LENGTH 150mm

Table 4.9 shows the results is tabulated for experimental and theoretical value for circular PVC tube with length 150mm. The percentage of error for energy absorbed, mean load and plastic folding are calculated. From theoretical studies conducted by Singace, the percentage error for energy absorbed for sample 1, sample 2 and sample 3 are 29.10%, 26.20% and 24.90% respectively. According to this results, the difference between experimental and theoretical results is very large but still acceptable as long as not more than 35% or error. The progressive deformation for all three sample produced a quite large different for energy absorbed between experimental and theoretical value due to highest plastic deformation of the tubes (ductility). In addition, ductile materials absorbed more energy compared with brittle materials

Besides, for the mean load, the percentage of error for sample 1, sample 2 and sample 3 are 29.10%, 26.30% and 24.90% respectively. The result shows a very large of different between experimental and theoretical value. According to Singace theorem, the mean load is depends on the energy absorbed because deformation for this testing is constant which is 90mm. The relationship between energy absorbed and mean load is directly proportional. So, if the error for energy absorbed increased, the error for mean load also will be increased. It clearly can be seen from the percentage of error for sample 1 which is has highest error for both energy absorbed and mean load.

Next, the percentage of error for plastic folding shows very close error. For sample 1, sample 2 and sample 3, the error that has been calculated using Singace theorem are 9.16%, 7.97% and 6.37% respectively. The close result of error is due to progressive deformation for all three tubes. So, based on theoretically, the total of fold that should happened is around 3 or 4 folds.

Table 4. 9: Comparison between experimental and theoretical results of quasi-static testing for PVC tube with length 150mm

| Sample   | Max load (kN) | Compression stress at max load (MPa) | Compressive extension at max load (mm) | Experimental               |                      |                           | Theoretical                 |            |                       |            |                       |            |
|----------|---------------|--------------------------------------|--|----------------------------|----------------------|---------------------------|-----------------------------|------------|-----------------------|------------|-----------------------|------------|
|          |               |                                      |  | Total area under graph (J) | Mean load, $P_m$ (N) | Plastic folding, 2Hm (mm) | Total area under graph (kJ) | % of error | Mean load, $P_m$ (kN) | % of error | Plastic folding, (mm) | % of error |
| Sample 1 | 27.09         | 52.57                                | 4.96                                   | 758.64                     | 8429.91              | 22.80                     | 1.07                        | 29.10      | 11.89                 | 29.10      | 25.10                 | 9.16       |
| Sample 2 | 27.05         | 52.49                                | 4.98                                   | 789.15                     | 8768.61              | 23.10                     | 1.07                        | 26.20      | 11.89                 | 26.30      | 25.10                 | 7.97       |
| Sample 3 | 27.52         | 53.40                                | 4.86                                   | 803.90                     | 8932.82              | 23.50                     | 1.07                        | 24.90      | 11.89                 | 24.90      | 25.10                 | 6.37       |

#### 4.4.7 CIRCULAR PVC TUBE WITH LENGTH 200mm

For circular PVC tube with same thickness and outer diameter but different in length which is 200mm are deformed in diamond mode for sample 1 and sample 3. But, for sample 2, the tube is suddenly break at a top part of the tube during a testing at deformation of 6.9mm as shown in Figure 4.16. Figure 4.17 shows the load displacement curve for sample 1 obtained from the experimental work. The graph shows a five highest peaks, means that the tube produce five folds. The series picture of progressive deforming mode of the tube for sample 1 are shown in Figure 4.18.

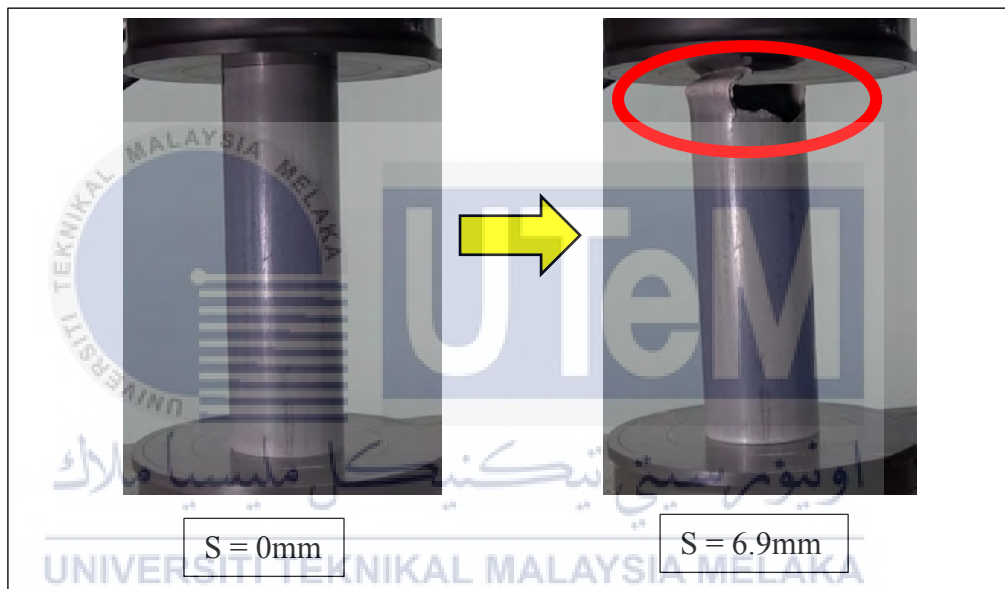


Figure 4. 16: Global buckle for sample 2 with length 200mm

Based on Figure 4.17, the first peak which is maximum load or  $P_{\text{peak}}$  where the tube is started to fold at deformation of 6.43mm. The value of  $P_{\text{peak}}$  for this sample is 27.33 kN. The load is decreased to 3.6 kN at 10mm it deformed as shown at picture S1. Then, this load increase for the second highest peak which is 13.9 kN at deformation of 27mm as shown at picture S3. At this point, this tube started to produce a second fold.

After that, the load is drop back to 5.0 kN at deformation of 40mm as shown at picture S4. For this point, the tube already produced 2 folds. Next, the load increase again until reached a point 10.5 kN as a starting point to produce a third fold at deformation of 51mm. Then, the load dropped again until 3.9 kN at deformation of 69mm as shown at picture S7.

At this point, the tube has produced 3 completed fold. The load continued to increase drastically until reached 12.4 kN at deformation of 82mm as shown at picture S8.

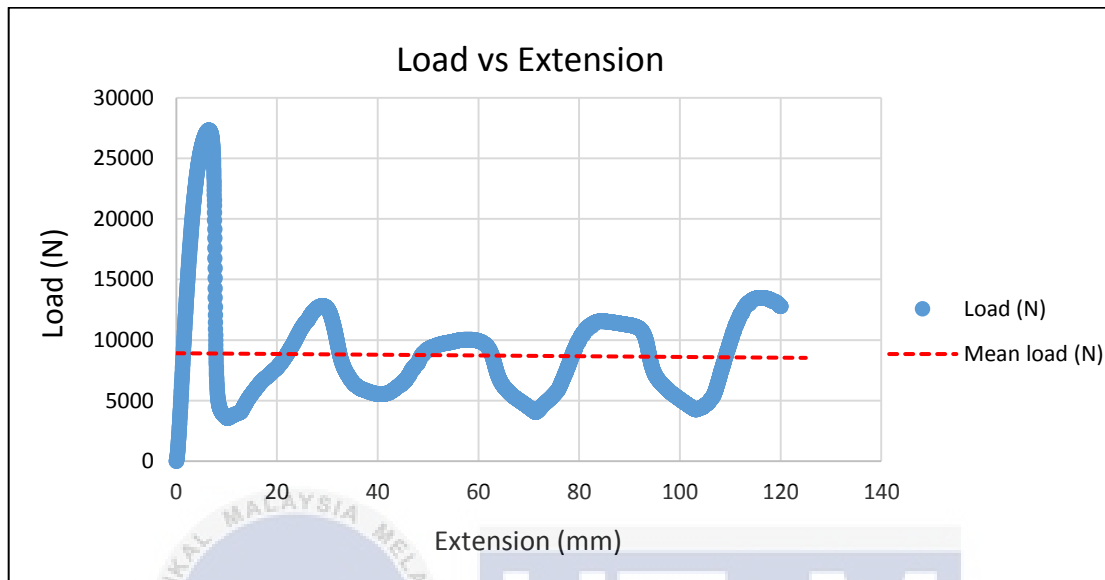


Figure 4. 17: Sample 1 of load displacement curve for PVC tube with length 200mm

Next, the load dropped again until 4.2 kN at deformation of 103mm as shown at picture S10. The tubes already produced a 4 completed folds. The testing is continued again until the load increased to 14.2 kN at deformation of 112mm as shown at picture S11. Same phenomenon occurred where the load is decreased slightly due to producing a fold until a point of 12.8 kN at deformation 120mm as shown at picture S12.

The testing stop at that point because already reached the point of 60% from the total length of the tube which is 120mm. As a conclusion, the progressive deformation of sample 1 for PVC tube with length 200mm has produced up to 5 completed folds.



Figure 4. 18: Sample 1 of deforming mode for PVC tube with length 200mm

#### 4.4.7.1 COMPARISON BETWEEN EXPERIMENTAL AND THEORETICAL VALUE FOR PVC TUBE WITH LENGTH 200mm

Table 4.10 shows the results is tabulated for experimental and theoretical value for circular PVC tube with length 200mm. The percentage of error for energy absorbed, mean load and plastic folding are calculated. From the experimental work, sample 2 has undergo global buckling at deformation 6.9mm. So, the value of energy absorbed, mean load and plastic folding for this sample are unacceptable. This sample 2 are considered as rejected sample due to global buckling. From theoretical studies conducted by Singace, the percentage error for energy absorbed for sample 1 and sample 3 are 25.20% and 32.00% respectively. According to this results, the difference between experimental and theoretical results is very large but still acceptable as long as not more than 35% or error. The progressive deformation for both sample 1 and sample 3 produced a quite large different for energy absorbed between experimental and theoretical value due to highest plastic deformation of the tubes (ductility). In addition, ductile materials absorbed more energy compared with brittle materials

Besides, for the mean load, the percentage of error for sample 1 and sample 3 are 25.10% and 31.08% respectively. The result also shows a very large of different between experimental and theoretical value. According to Singace theorem, the mean load is depends on the energy absorbed because deformation for this testing is constant which is 120mm. The relationship between energy absorbed and mean load is directly proportional. So, if the error for energy absorbed increased, the error for mean load also will be increased. It clearly can be seen from the percentage of error for sample 3 which is has highest error for both energy absorbed and mean load.

Next, the percentage of error for plastic folding shows quite close of percentage error. For sample 1 and sample 3, the error that has been calculated using Singace theorem are 10.36% and 11.55% respectively. The resulted of error is due to progressive deformation for both sample of tubes. It produced highest plastic deformation along circumference of the tubes and also at middle part of the folding. So, based on theoretically, the total of fold that should happened is around 4 or 5 folds.



Table 4. 10: Comparison between experimental and theoretical results of quasi-static testing for PVC tube with length 200mm

| Sample   | Max load (kN) | Compression stress at max load (MPa) | Compressive extension at max load (mm) | Experimental               |                      |                           | Theoretical                 |            |                       |            |                       |            |       |
|----------|---------------|--------------------------------------|--|----------------------------|----------------------|---------------------------|-----------------------------|------------|-----------------------|------------|-----------------------|------------|-------|
|          |               |                                      |  | Total area under graph (J) | Mean load, $P_m$ (N) | Plastic folding, 2Hm (mm) | Total area under graph (kJ) | % of error | Mean load, $P_m$ (kN) | % of error | Plastic folding, (mm) | % of error |       |
| Sample 1 | 27.33         | 53.05                                | 6.43                                   | 1069.21                    | 8910.83              | 22.50                     | 1.43                        | 25.20      | 11.89                 | 25.10      | 10.36                 | 25.10      | 10.36 |
| Sample 2 | 26.41         | 51.25                                | 5.88                                   | -                          | -                    | -                         | 1.43                        | -          | 11.89                 | -          | -                     | 25.10      | -     |
| Sample 3 | 26.01         | 50.47                                | 5.80                                   | 972.38                     | 8103.84              | 22.20                     | 1.43                        | 32.00      | 11.89                 | 31.08      | 11.55                 | 25.10      | 11.55 |

#### 4.4.8 SAMPLE CALCULATION FOR CIRCULAR PVC TUBES

The energy absorbed, mean load and plastic folding is calculated using Singace theorem. The value of tensile stress at yield, outer diameter and thickness of tubes are tabulated in Table 4.11. The value of tensile stress at yield is gained from tensile test.

Table 4. 11: Properties of circular PVC tubes

| Tensile stress at yield, $\sigma_u$<br>(MPa) | Outer diameter, d<br>(mm) | Thickness of tube, t<br>(mm) |
|--|---------------------------|------------------------------|
| 24.14  | 60.2                      | 2.9                          |

From the previous studies, the equation given are :

For mean load,  $P_m$  :

$$P_m = M_o \left( -\frac{\pi}{3}N + \frac{2\pi^2}{N} \tan \left( \frac{\pi}{2N} \right) \frac{D}{t} \right) \quad (4.5)$$

$$P_m = \frac{\sigma_u t^2}{2\sqrt{3}} \left( -\frac{\pi}{3}N + \frac{2\pi^2}{N} \tan \left( \frac{\pi}{2N} \right) \frac{D}{t} \right) \quad (4.6)$$

The phenomenon of lobar buckling showing modes where  $N = 2$  (Little et al., 2010).

$$P_m = \frac{(24.14 \times 10^6)(0.0029)^2}{2\sqrt{3}} \left( -\frac{\pi}{3}(2) + \frac{2\pi^2}{2} \tan \left( \frac{\pi}{2(2)} \right) \frac{(0.0602)}{0.0029} \right)$$

$$P_m = 11.89 \text{ kN}$$

For half plastic folding,  $H_m$  :

$$H_m = 0.95 \sqrt{dt} \quad (4.7)$$

$$H_m = 0.95 \sqrt{(0.0602)(0.0029)}$$

$$H_m = 12.55 \text{ mm}$$

So, for one completed plastic folding is,  $2H_m = 25.10 \text{ mm}$

For energy absorbed :

$$E = P_m \times \text{deformation, } S \quad (4.8)$$

1) For 100mm length of tube, deformation,  $S = 60\text{mm}$

$$E = (11.89 \times 10^3) \times 0.06$$

$$E = 713.1 \text{ J}$$

2) For 150mm length of tube, deformation,  $S = 90\text{mm}$

$$E = (11.89 \times 10^3) \times 0.09$$

$$E = 1.07 \text{ kJ}$$

3) For 200mm length of tube, deformation,  $S = 120\text{mm}$

$$E = (11.89 \times 10^3) \times 0.12$$

$$E = 1.43 \text{ kJ}$$

For percentage of error, % :

$$\% \text{ error} = \frac{\text{experimental value} - \text{theoretical value}}{\text{theoretical value}} \times 100\% \quad (4.9)$$

Example calculation for percentage of error for mean load, energy absorbed and plastic folding for 100mm length of tube (sample 1) are shown below, respectively.

$$4) \% \text{ error} = \left| \frac{9143.32 - 11890}{11890} \right| \times 100\% \quad (4.10)$$

$$\% \text{ error} = 23.10 \%$$

$$5) \% \text{ error} = \left| \frac{548.79 - 713.1}{713.1} \right| \times 100\%$$

$$\% \text{ error} = 23.00 \%$$

$$6) \% \text{ error} = \left| \frac{23.5 - 25.1}{25.1} \right| \times 100\%$$

$$\% \text{ error} = 6.37 \%$$

#### 4.5 PAPER MODEL FOR SQUARE ALUMINIUM TUBE

The deforming mode for a square aluminium tube is demonstrated in a series of photographs of paper models shown in Figure 4.20. It shows a various stage of the deformation process. The paper model shows only one completed folding for square aluminium tube. The deformation is concentrated at hinges of the tubes. In addition, as shows in Figure 4.19, the top and bottom part of the tubes is remain flat throughout the deformation. It produced a rectangular shape in the middle of the tubes after a compression testing. Note also that the deforming mode for a longer tube is assumed to have a series of collapse mode occurred one after another.

Besides, the deforming mode of tube contains two types of hinges which is fixed horizontal hinges and inclined travelling hinges. The horizontal plastic hinges occurred at the middle part of the tube. The direction of the hinges is perpendicular to the applied compression load. Furthermore, the plastic zone concentrated at the point of hinges. Two horizontal hinges on opposite sides move outwards while hinges on adjacent sides move inwards. For the inclined hinges, the plastic hinges originate from four corners of the tube to finish about  $45^\circ$  to the horizontal plastic hinges in the completely folding of the tubes.

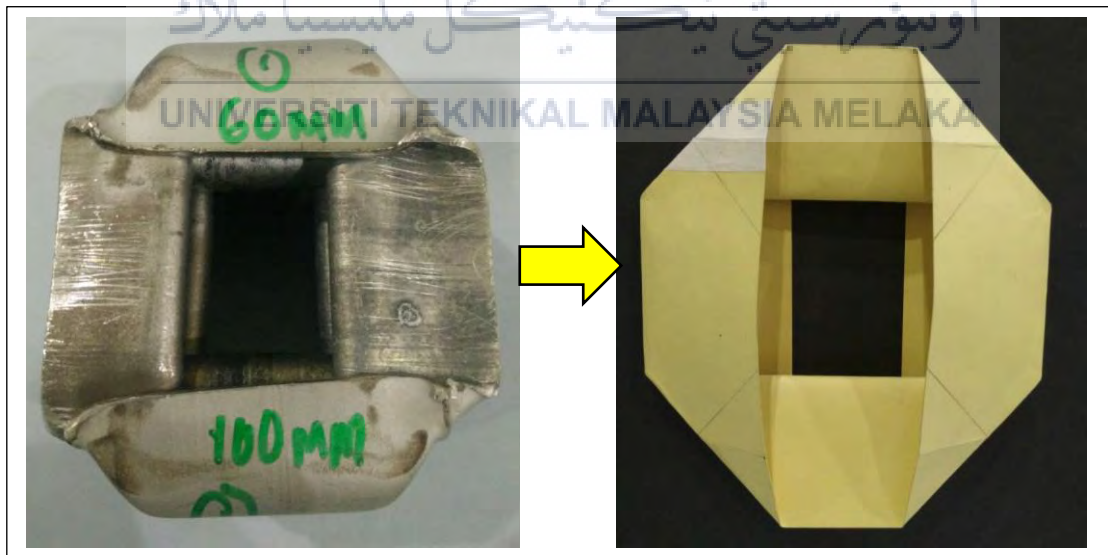


Figure 4. 19: Top view of tube and paper model



Figure 4. 20: Series of photographs of paper models

## CHAPTER 5

### CONCLUSION AND RECOMMENDATION

#### 5.1 INTRODUCTION

This chapter discuss about the finding from this study. There are two types of materials has been selected which is aluminium and polyvinyl chloride (PVC) tubes. The literature study is to review the mechanical properties of the selected materials (aluminium and PVC), quasi static testing, energy absorption, mean load, plastic folding, type of deforming modes and paper models of deforming modes using a thick paper.

#### 5.2 CONCLUSION

In this study, square aluminium and circular PVC tubes is studied. Therefore, the tensile test is performed in order to determine the mechanical properties of the selected materials. The value such as tensile stress at yield is used in calculation of mean load for theoretically value. The tensile stress at yield obtained from the tensile test for aluminium and PVC tubes are 159.081 MPa and 24.142 MPa respectively.

Then, second testing has been carried out which is quasi static test on both tubes. There are three different in length for each type of tubes which are 100mm, 150mm and 200mm has been tested under this quasi static testing. The experimental results such as

energy absorption, mean load and plastic folding are compared with theoretical results. The comparison of results shows a good agreement between them.

For both tubes, the type of deforming modes obtained are diamond mode. The number of plastic folding is increased due to increase in length of the tubes. The length of the plastic folding for PVC tubes is longer compared with aluminium tubes due to ductility behaviour. The deforming modes for square aluminium tube which is diamond mode is modelling using a thick paper. The movement of the plastic hinges is study in order will be used as reference in modelling of paper model.

Finally, the photographs a series of paper model is prepared to show the movement of plastic hinges and the phenomenon of compression process. Last but not least, the paper model will be used as teaching tools in order to increase the understanding on deforming mode of square aluminium tubes under quasi static loading.

### 5.3 RECOMMENDATION

Based on the conclusion in this study, further research can be conducted by the following:

- i. – Changing the variables such as dimension of the tubes, type of compression test such as dynamic test and type of material of the tubes.
- ii. Conduct a hardness test in order to obtain the mechanical properties of the selected materials.
- iii. Using a finite element analysis software as proposed to compare between experimental and theoretical results.
- iv. Develop a paper model of deforming mode for circular tube.

## REFERENCES

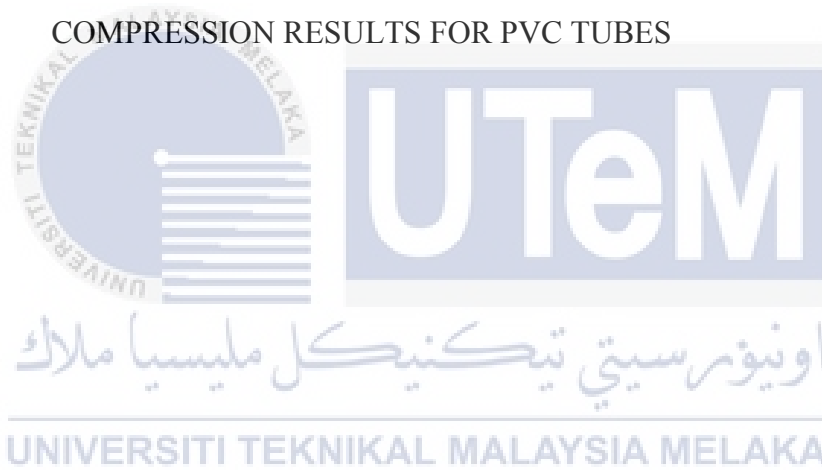
- Ahmad, Z. (2009). Impact and Energy Absorption of Empty and Foam-filled Conical Tubes, (December).
- Alghamdi, A. A. A. (2001). Collapsible impact energy absorbers: An overview. *Thin-Walled Structures*, 39(2), 189–213. [https://doi.org/10.1016/S0263-8231\(00\)00048-3](https://doi.org/10.1016/S0263-8231(00)00048-3)
- Alhamati, A., & Ghazali, A. (2007). Investigation on the Behavior of Rigid Polyvinylchloride Pipes Subjected to Uniaxial Compression Loads. *ASEAN Journal on ...*, 3(7), 1916–1923. Retrieved from <http://203.191.52.20/index.php/ASEAN/article/viewArticle/416>
- Andrews, K. R. F., England, G. L., & Ghani, E. (1983). Classification of the axial collapse of cylindrical tubes under quasi-static loading. *International Journal of Mechanical Sciences*, 25(9–10), 687–696.
- ASTM Int. (2009). Standard Test Methods for Tension Testing of Metallic Materials 1. *Astm*, (C), 1–27. <https://doi.org/10.1520/E0008>
- ASTM International. (2003). Standard test method for tensile properties of plastics. *ASTM International*, 8, 46–58. Retrieved from <http://scholar.google.com/scholar?hl=en&btnG=Search&q=intitle:Standard+Test+Method+for+Tensile+Properties+of+Plastics#0>
- Christy Albert, P., Radzi Ab Ghani, A., Zaid Othman, M., & Ahmad Zaidi, A. M. (2016). Axial Crushing Behavior of Aluminum Square Tube with Origami Pattern. *Modern Applied Science*, 10(2), 90. <https://doi.org/10.5539/mas.v10n2p90>
- Ejlertsson, J., Horsing, M., & Mersiowsky, I. (2000). Behaviour of PVC Products in Landfilled Municipal Solid Waste at Different Temperatures.
- JUNNING SUN, B. E. (2000). Prediction of energy absorption of extruded tubes.



- Little, A. P. F., Ross, C. T. F., Flowers, D., Brown, G. X., & Arndt, S. (2010). A theoretical and experimental investigation of externally ring-stiffened cylindrical pressure vessels subjected to external pressure.
- Ma, J. (2011). Thin-walled Tubes with Pre-folded Origami Patterns as Energy Absorption Devices, 194.
- Meng, Q., Al-Hassani, S. T. S., & Soden, P. D. (1983). Axial crushing of square tubes. *International Journal of Mechanical Sciences*, 25(9–10), 747–773.  
[https://doi.org/10.1016/0020-7403\(83\)90080-2](https://doi.org/10.1016/0020-7403(83)90080-2)
- Miyazaki, M., & Negishi, H. (2003). Deformation and Energy Absorption of Aluminum Square Tubes with Dynamic Axial Compressive Load. *Materials Transactions*, 44(8), 1566–1570. <https://doi.org/10.2320/matertrans.44.1566>
- Pled, F., Yan, W., & Wen, C. (2007). Crushing modes of aluminium tubes under axial compression. *Proceedings of the 5th Australasian Congress on Applied Mechanics: 10-12 December 2007, Brisbane, Australia*, (December), 178–183.
- Sheasby, P. G., & Pinner, R. (2001). The Surface Treatment and Finishing of Aluminum and its Alloys, 2, 417–462.
- Tai, Y. S., Huang, M. Y., & Hu, H. T. (2010). Axial compression and energy absorption characteristics of high-strength thin-walled cylinders under impact load. *Theoretical and Applied Fracture Mechanics*, 53(1), 1–8.  
<https://doi.org/10.1016/j.tafmec.2009.12.001>
- Timoshenko. (1961). Finite Element Study of Energy Absorption Characteristics of a Hybrid Structure - Composite Wrapped on a Square Metal Tube, (May), 60. Retrieved from <https://www.researchgate.net/publication/33719500>
- Trondheim. (2005). Behaviour of aluminium extrusion subjected to axial loading.

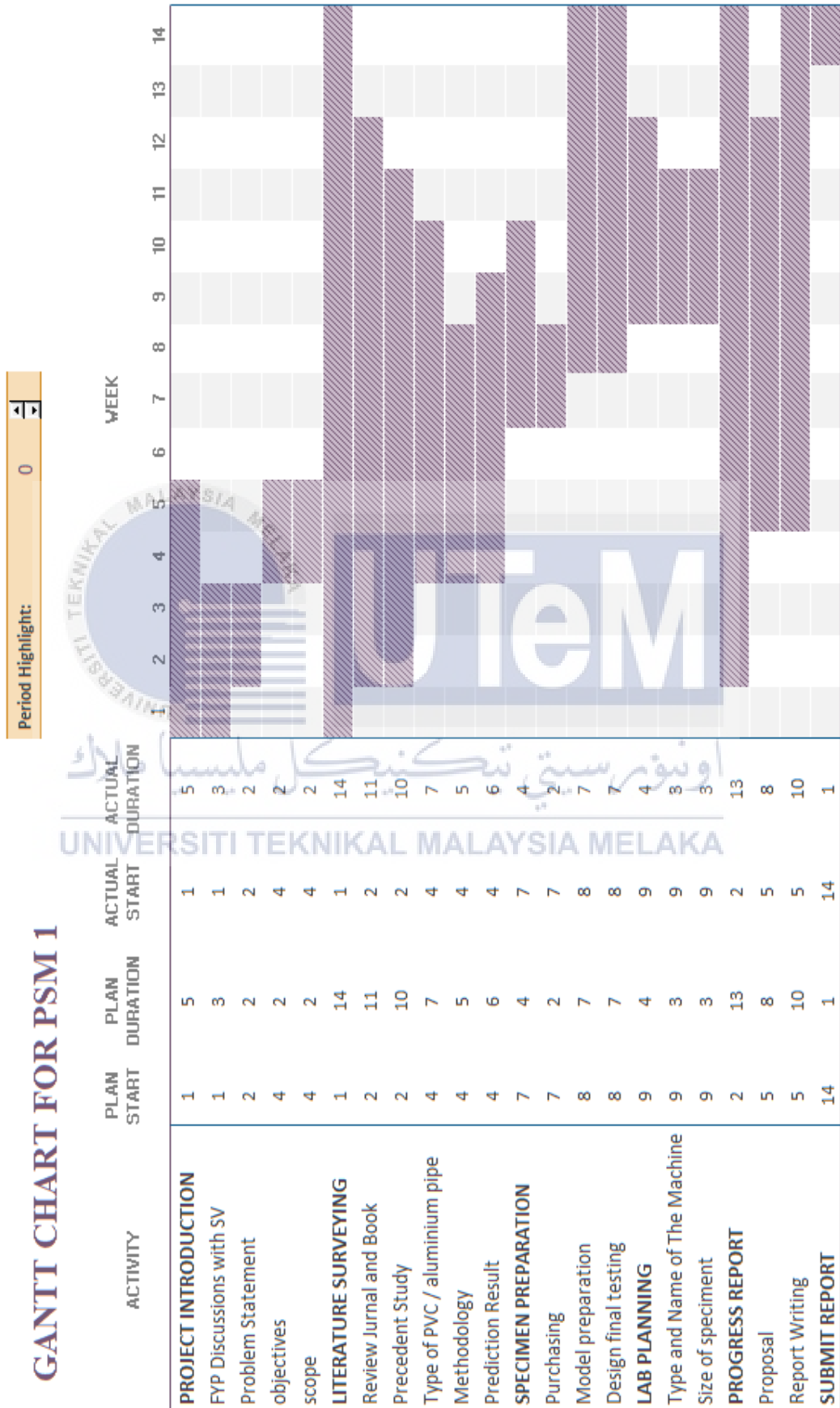
## LIST OF APPENDICES

| APPENDIX | TITLE                                   | PAGE |
|----------|---|------|
| A        | GANTT CHART FOR PSM 1                   | 74   |
| B        | GANTT CHART FOR PSM 2                   | 75   |
| C        | COMPRESSION RESULTS FOR ALUMINIUM TUBES | 76   |
| D        | COMPRESSION RESULTS FOR PVC TUBES       | 78   |



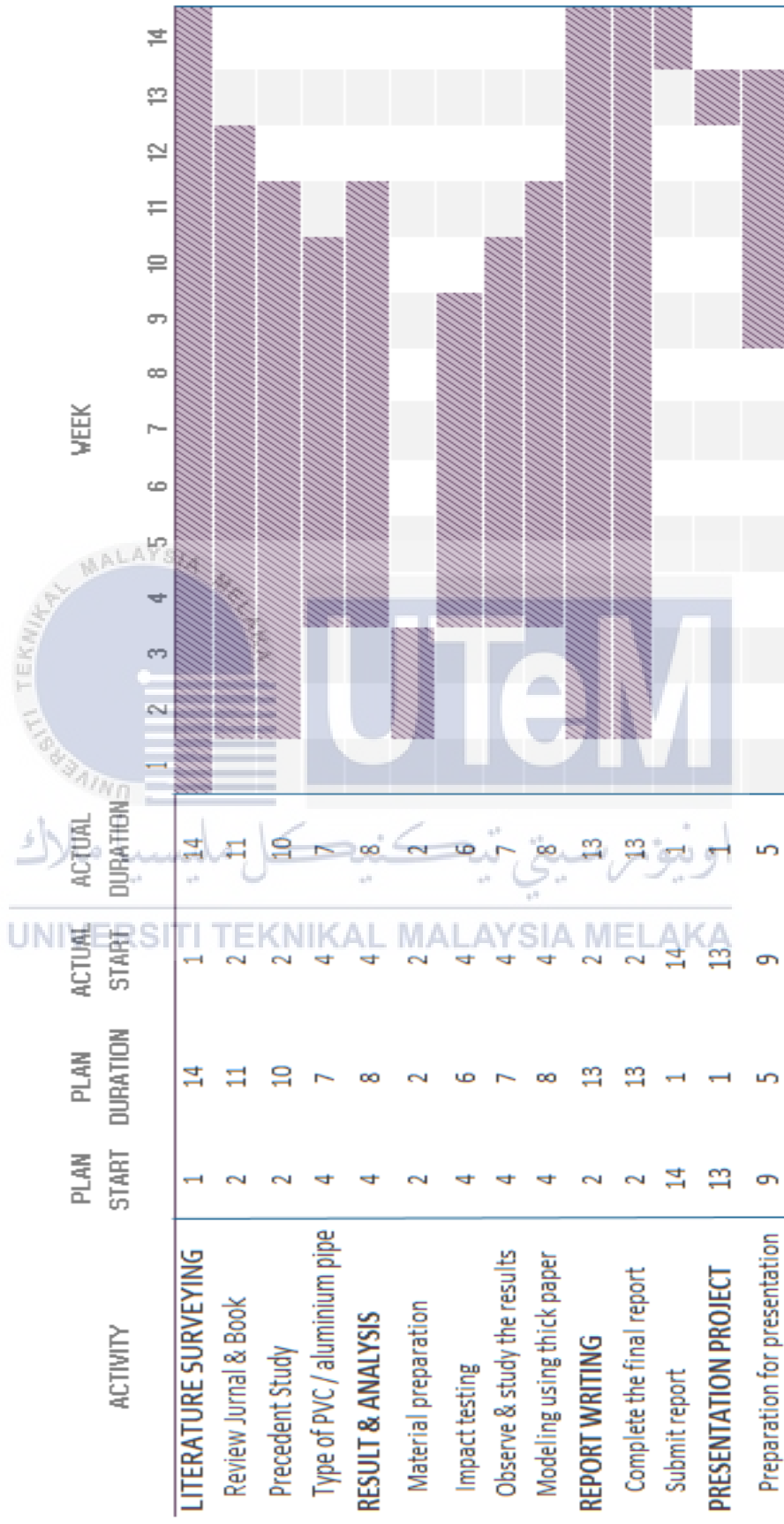
APPENDIX A : GANTT CHART FOR PSM 1

GANTT CHART FOR PSM 1

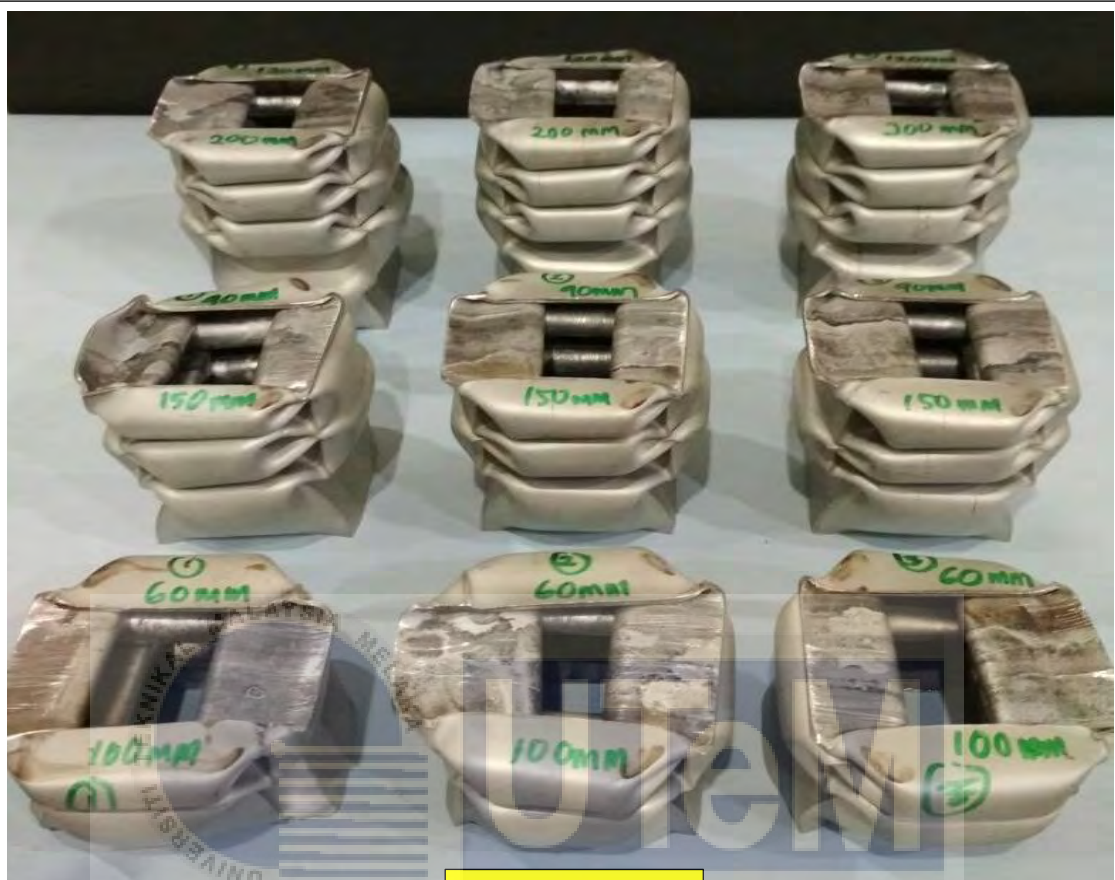


APPENDIX B : GANTT CHART FOR PSM 2

GANTT CHART FOR PSM 2



**APPENDIX C : COMPRESSION RESULTS FOR ALUMINIUM TUBES**



**TOP VIEW**

اونيورسيتي تېكنيكل مليسيا ملاك

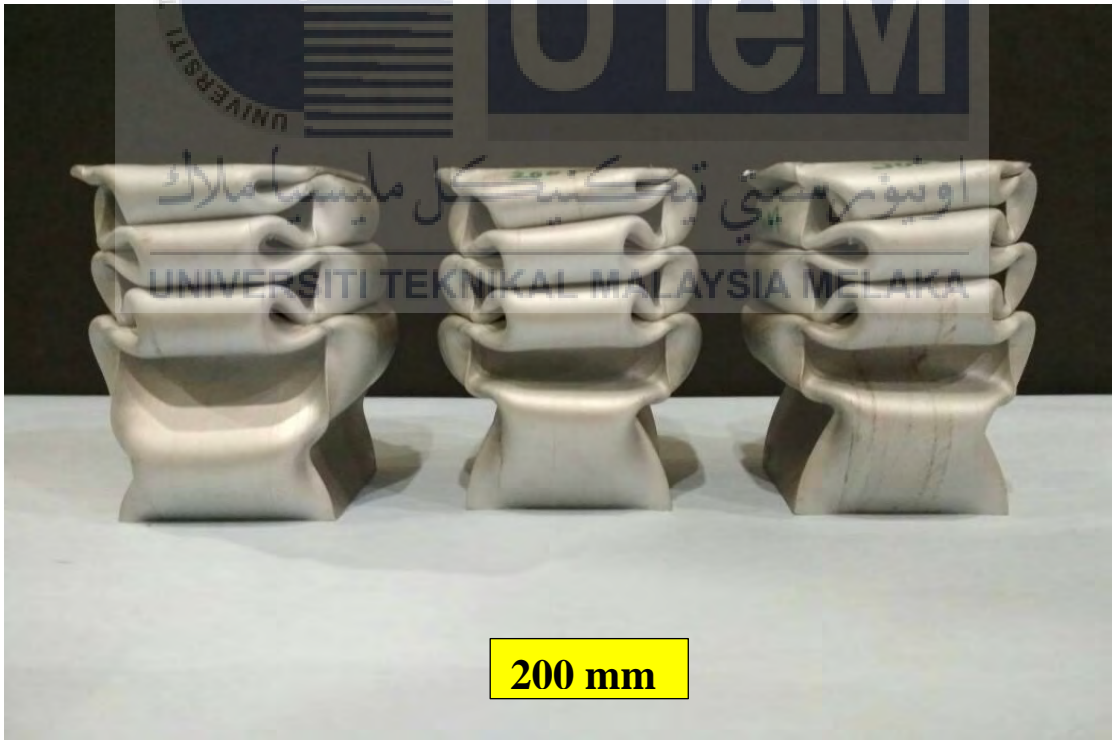
UNIVERSITI TEKNIKAL MALAYSIA MELAKA



**100 mm**



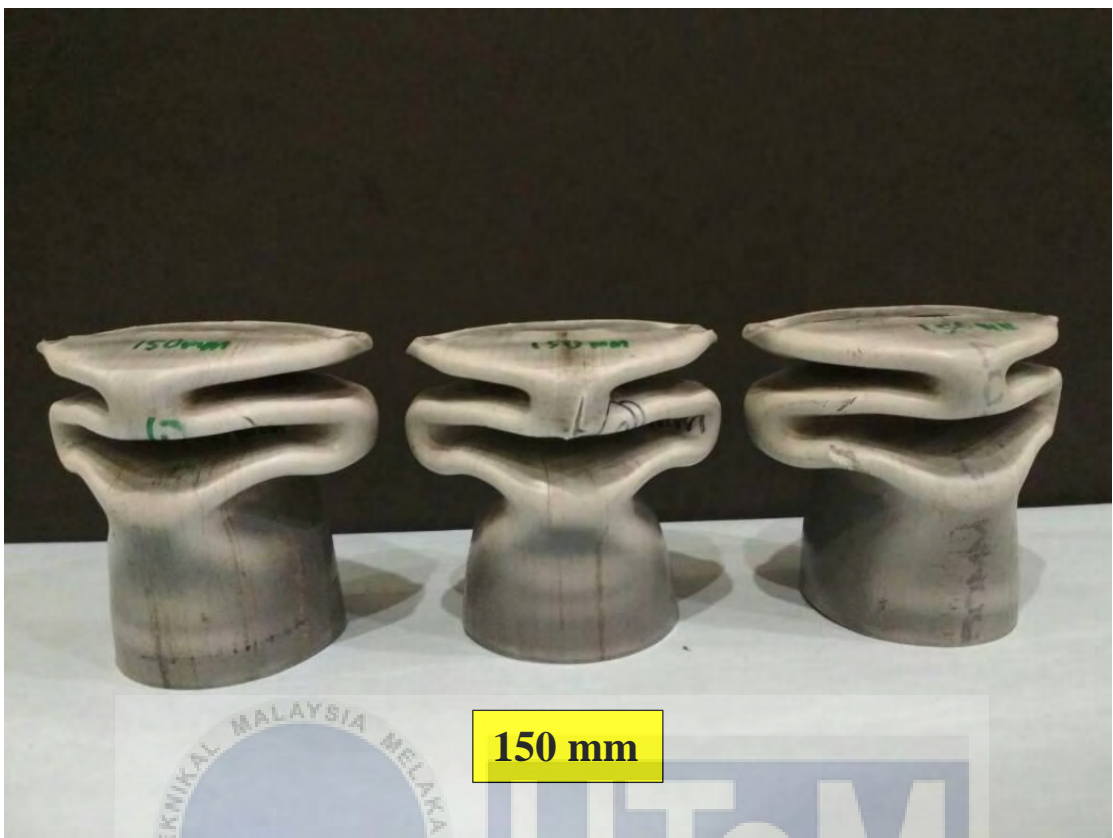
150 mm



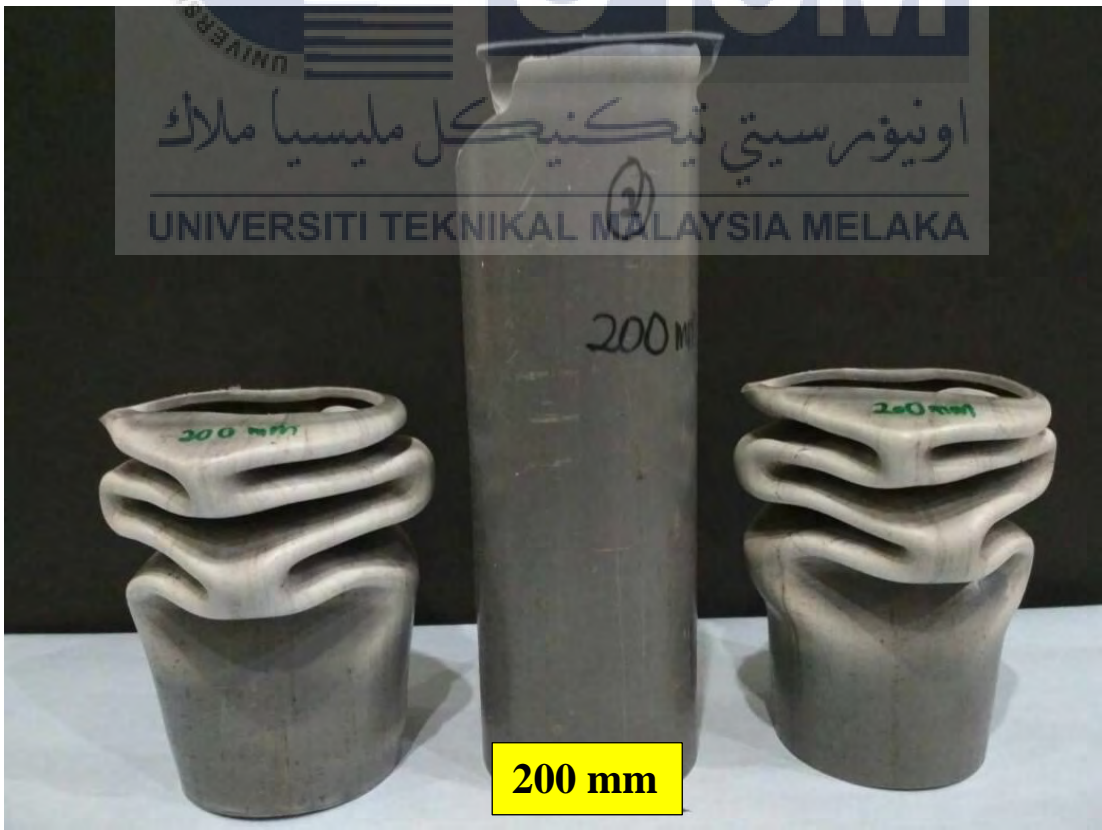
200 mm

**APPENDIX D : COMPRESSION RESULTS FOR PVC TUBES**





150 mm



200 mm